NASA TM-81635

NASA Technical Memorandum 81635

NASA-TM-81635 19820012070

Effect of Facility Variation on the Acoustic Characteristics of Three Single Stream Nozzles

Orlando A. Gutierrez
Lewis Research Center
Cleveland, Ohio

Prepared for the
One-hundredth Meeting of the Acoustical Society of America
Los Angeles, California, November 17-21, 1980

NASA

34,000 ppm of unsupported radiogenic lead. This basal conglomerate must
ENTER:

3 1 1 RN/NASA-TM-81635
4 1 1 RN/NASA-TM-81635
DISPLAY 04/2/1
82N19944** ISSUE 10 PAGE 1428 CATEGORY 71 RPT#: NASA-TM-81635
E-646 80/00/00 38 PAGES UNCLASSIFIED DOCUMENT
UTTL: Effect of facility variation on the acoustic characteristics of three single stream nozzles
AUTH: A/GUTIERREZ, O. A.
CORP: National Aeronautics and Space Administration. Lewis Research Center, Cleveland, Ohio. AVAIL.NTIS SAP: HC A03/MF A01
Presented at the 100th Meeting of the Acoust. Soc. of Am., Los Angeles, 17-21 Nov. 1980
MAJS: /*ACOUSTIC PROPERTIES/*JET AIRCRAFT NOISE/*NOISE MEASUREMENT/*NOZZLE GEOMETRY
MINS: / CONICAL NOZZLES/ CONVERGENT NOZZLES/ FAR FIELDS/ MICROPHONES/ NOZZLE FLOW
ABA: Author
ABS: The characteristics of the jet noise produced by three single stream

EFFECT OF FACILITY VARIATION ON THE ACOUSTIC CHARACTERISTICS OF THREE SINGLE STREAM NOZZLES

BY Orlando A. Gutierrez

National Aeronautics and Space Administration
Lewis Research Center
Cleveland, Ohio 44135

ABSTRACT

The characteristics of the jet noise produced by three single stream nozzles have been investigated statically at the NASA-Lewis Research Center outdoor jet acoustic facility. The nozzles consisted of a 7.6 cm diameter convergent conical, a 10.2 cm diameter convergent conical and an 8-lobe daisy nozzle with 7.6 cm equivalent diameter flow area. The same nozzles have been tested previously at cold flow conditions in other facilities such as the Royal Aircraft Establishment (RAE) 7.3 m acoustic wind tunnel. The acoustic experiments at NASA covered pressure ratios from 1.4 to 2.5 at total temperatures of 811 K and ambient. The data obtained with four different microphone arrays are compared. The results are also compared with data taken at the RAE facility and with a NASA prediction procedure (i.e., Stone and Montegani (1980)).

E-646

INTRODUCTION

The NASA-Lewis Research Center outdoor jet acoustic facility has been used by various investigators to obtain far field static jet noise data on a variety of nozzle configurations. These studies have covered single-stream and dual-stream nozzles suitable to such diverse applications as short take-off and landing aircraft (ref. 1), conventional aircraft (ref. 2), and future supersonic transports (refs. 3 and 4). The nozzle models used in these investigations have varied in size from 5 to 20 cm in diameter, with jet total temperatures ranging from ambient to 1085 K, and with various microphones arrays used for obtaining the far field noise measurements. It is important, therefore, to assess the possible effect of the microphone array variation on the results obtained.

Another concern that arises when comparing experimental jet noise data from several facilities is the repeatability of results from one test site to another. In order to resolve this concern, the same experimental nozzles can be tested in various acoustic facilities and the results compared.

This paper presents the results of a program conducted at the NASA Lewis Research Center outdoor jet acoustic facility to determine the effect of four microphone arrays upon the jet noise data obtained from three different nozzles which had been previously tested at other facilities. The microphone arrays consisted of the following: 3 m sideline array consisting of microphones at ground level (for low frequencies) and microphones mounted at the nozzle centerline (for high frequencies) with all the microphones located over a hard surface; a 7 m sideline array similar to the 3 m array; a 4.6 m polar array of microphones level with the nozzle centerline mounted above a noise absorbing (acoustic foam) surface; and a 4.6 m polar array of

microphones mounted on a boom located in the vertical plane of the nozzle axis and over a noise absorbing surface. The three test nozzles consisted of a 7.6 cm diameter convergent conical nozzle, a 10.2 cm diameter convergent conical nozzle and a 7.6 cm equivalent diameter 8-lobe nozzle. All three of these nozzles were on loan from the National Gas Turbine Establishment (NGTE). These nozzles have already been tested statically and under simulated flight conditions at the Royal Aircraft Establishment (RAE) 7.3 m wind tunnel (refs. 5 and 6), using cold air flow.

The results of the acoustic experiments conducted with the three nozzles at pressure ratios varying from 1.4 to 2.5 and at ambient and 811 K total temperatures at the NASA acoustic facility are presented herein. Overall sound pressure level (OASPL) directivity and sound pressure level (SPL) spectra are compared for the various microphone arrays with cold flow results from the previous tests at RAE and with a prediction procedure (ref. 7).

SYMBOLS

A	nozzle exit area
c_o	speed of sound at ambient temperature
f	1/3 octave band center frequency
M	jet Mach number
M_c	convective Mach number, $0.62\ (V_j/c_o)$
OASPL	Overall sound pressure level, dB re 20 $\mu N/m^2$
$OASPL_{exp}$	measured value of OASPL
$OASPL_{calc}$	calculated value of OASPL, using method of reference 7
OASPL*	predicted OASPL factor (eq. (1))
PR	nozzle pressure ratio
R	nozzle exit to microphone distance
R_c	corrected noise source to microphone distance
RH	ambient relative humidity
ST. DEV.	standard deviation
SPL	1/3-octave-band sound pressure level, dB re 20 $\mu N/m^2$
T_o	ambient temperature
T_T	jet total temperature
V_j	jet velocity, calculated from upstream data
V_p	jet velocity, measured by traversing probe at nozzle exit
X_θ	source location distance
α	turbulence length scale ratio, used as $\alpha = 0.2$
Δ	OASPL difference, $OASPL_{exp} - OASPL_{calc}$, dB
Δ_{mean}	mean value of Δ, dB
θ	angle measured from nozzle inlet, deg

θ_c	corrected angle, measured from noise source location, deg (ref. 7)
ρ_j	density of jet stream at fully expanded conditions
ρ_o	density of air at ambient conditions
ω	density exponent (ref. 7)

APPARATUS AND PROCEDURE

Facility

A photograph of the NASA Lewis outdoor jet acoustic facility is shown in figure 1. This is a dual independent stream facility in which coannular nozzles can be tested; however, for this program only the straight-through leg of the flow system was used. The flowline has its own air and fuel flow control and measuring systems. The air is heated with a jet engine single-can combustor. A muffler attenuates the flow control valve noise and internal combustion noise. The system is designed to give a maximum nozzle exhaust temperature of 1100 K and nozzle pressure ratios up to 3.0. The facility axis is parallel and 1.7 m above the ground plane of the test area. The ground plane is composed of asphalt interspersed with patches of concrete. A two section adapter (fig. 2) was used as a transition from the 33 cm inside diameter muffler exit flange to the 20.3 cm inside diameter at the upstream end of the test nozzles. The location of the pressure and temperature rakes used to define the nozzle operating conditions is shown in figure 2. Also shown in figure 2 is a flow screen mounted between the transition pipe and the nozzle entrance. This flow screen had been used as a flow straightener in previous tests at the RAE for all the configurations but was only used for one series of tests in this program. The nozzles and adapters were covered with thermal insulation to minimize temperature losses between the metering station and the nozzle exit.

Test Nozzles

Three different single stream test nozzles were used in this program: a 10.2 cm diameter convergent conical nozzle, a 7.6 cm diameter convergent conical nozzle and a 7.6 cm equivalent diameter 8-lobe nozzle. All of the nozzles are the property of the NGTE and were on loan for this program. These nozzles have also been tested at the RAE 7.3 m wind tunnel and at the NASA-Ames Research Center 12x24 meter wind tunnel.

The 10.2 cm diameter conical nozzle is shown in figure 3. The thermocouples shown on the outer wall upstream of the nozzle exit were added by NASA to allow corrections to be made to the nozzle area based on skin temperature. This nozzle had a blunt lip approximately 0.16 cm thick. The inside wall of the nozzle has a constant taper of 8° throughout its entire length.

The 7.6 cm diameter conical nozzle is shown in figure 4. This nozzle had a sharp lip obtained by chamfering the nozzle outer wall. This nozzle has a nominal 10° taper throughout. The flange shown upstream of the nozzle exit is used to mount a smooth outer shield to allow testing of this nozzle in a moving air environment. The shield was not used for the present static tests.

The third nozzle consisted of the 8-lobe nozzle shown in figure 5. This nozzle had the same exit flow area as the 7.6 cm conical nozzle. The nozzle exit configuration is shown in figure 6. The nozzle consists of 8 deep lobes without a center plug. Each lobe is segmented into three sections by reinforcing plates. This nozzle also had provisions for an external shield (not used herein) to allow simulated flight tests.

Microphone Array Variations

Four different arrays were used to obtain the far field acoustic data gathered in this study, as described in the following paragraphs:

3 m sideline array. - In this array the microphones were placed at a constant 3.0 m distance from and parallel to the nozzle axis as shown in figures 7(a), (b) and 8. Microphones were mounted at the nozzle centerline height and at ground level. The centerline array consisted of 0.635 cm condenser microphones with the metal protective grids removed to improve the performance of the microphones at high frequencies. The ground level array consisted of 1.27 cm condenser microphones with the grids removed and placed 1 cm above grade at the equivalent acoustic ray locations as the corresponding centerline microphone. A photograph of the ground microphone installation is shown in figure 9. A total of 16 microphones was used, 8 centerline and 8 ground, located at angles of 30°, 60°, 90°, 110°, 130°, 140°, 150°, and 160° to the inlet axis measured from the exit plane of the nozzle. In this array, the microphones at each angle are at a different distance from the nozzle exit. All microphones were positioned to face the nozzle exit plane. The ground plane consisted of asphalt with interspersed concrete.

7.01 m sideline array. - The details of the 7.01 m sideline array are shown in figures 7(a) and (c). This array is similar to the 3 m sideline array with two exceptions: the microphones are at a constant 7.01 m distance from and parallel to the nozzle axis, and the 30° microphone position was replaced by a 40° position because of equipment interference.

4.57 m polar boom array. - This array, shown in figures 10 and 11, consisted of eight 0.635 cm condenser microphones without grids, mounted on a boom with the microphones placed on a vertical 4.57 m arc centered on the nozzle exit plane and located in the vertical axial plane of the nozzle. With this array, the ground plane was covered with 15.25 cm thick acoustic foam with an absorption coefficient of 1 down to a 0.4 kHz frequency. Microphones were located at angles of 30°, 60°, 90°, 110°, 130°, 140°, 150°, and 160° from the inlet axis of the nozzle.

4.57 m polar centerline array. - This array is also shown in figures 10 and 11 and is identical to the 4.57 m polar boom array, except that the microphones are mounted at the nozzle centerline height, 1.7 m above ground, rather than overhead. Data from the two polar arrays were obtained simultaneously, but were analyzed independently.

Procedure

Experimental. - Four different and independent sets of experiments were conducted:

1. Jet plume measurements for the conical nozzle were made in a plane 0.5 cm downstream of the nozzle exit with a probe capable of traversing in the axial direction as well as horizontally and vertically, as shown in fig-

ure 12. Details of the probe are shown in figure 13. This probe was calibrated in a wind tunnel at subsonic and supersonic speeds. Total temperature, total pressure and static pressure were measured. The plume survey apparatus was removed from the test site during the acoustic tests.

2. Acoustic measurements were made with the 3 m sideline array.

3. Acoustic measurements were made with the 7 m sideline array.

4. Simultaneous acoustic measurements were made with the 4.6 polar boom and 4.6 polar centerline arrays.

Steady state conditions were attained for each test before the data were recorded. Upstream total temperatures and total and static pressures were then automatically recorded as were the jet plume or acoustic data. For the acoustic tests, the noise signal from each microphone was sequentially analyzed on-line, and 1/3 octave band sound pressure levels were digitally recorded on magnetic tape for further processing. The noise signal from each microphone was also recorded unprocessed on F.M. magnetic tape. For the jet plume surveys, probe position, total temperature, total pressure and static pressure were automatically recorded.

Test matrix. - For each of the three test nozzles, data were obtained at nominal ambient and 811 K jet total temperatures for pressure ratios of 1.4, 1.75, 2.0 and 2.5. Repeat data were taken for each set at a 1.75 pressure ratio. All the preceding data were obtained without the flow straightening screen (fig. 2) upstream of the nozzle. However, one series was run with the 10.2 cm conical nozzle at ambient temperature with the screen installed.

Jet exhaust conditions. - Ideal nozzle exhaust velocities and Mach numbers were calculated from the measured upstream temperatures and pressures, assuming complete expansion to atmospheric conditions. The static temperatures were computed from the measured total temperatures after correcting the total temperature measurements for radiation heat losses (ref. 8).

Acoustic data reduction. - The method of reducing the acoustic data varied somewhat, depending on the microphone array. In order to convert the measured SPL values from the sideline arrays to the corresponding free-field values, the assumption was made that for each frequency the jet can be treated as a pure harmonic point source at the center of the nozzle exit plane and that the impedance of the ground plane is infinite. Ground reflection corrections were then calculated for each microphone location and frequency (ref. 9) and applied to the measured spectral data. Corrections for atmospheric attenuation of the noise signal were added to the spectral data, using the information from reference 10 to obtain lossless data. A single spectrum for each angle was obtained by combining the two sets of data obtained from the ground microphone and centerline microphone. The spectrum from the ground microphone was used over a frequency range from 100 to 2000 Hz and the spectrum from the centerline microphone was used over a frequency range from 5000 Hz to 80 KHz. The data from both microphones were arithmetically averaged over the intermediate frequency range from 2500 to 4000 Hz. For the data taken with both polar arrays, the assumption was made that the presence of the acoustic foam on the ground completely eliminated all reflections and that, in effect, the microphones were in the free field. Therefore, only the atmospheric attenuation correction was applied. Each of the polar arrays were handled as independent measurements; therefore, each microphone signal was used over the entire frequency range.

Jet plume data reduction. - For each point, flow-field properties were calculated from the measured data. The measured pressures (total and

static) were corrected for probe bow-shock effects, when necessary, according to reference 11. From these pressures the local Mach numbers were calculated. Total temperature measurements were corrected for thermocouple radiation losses (ref. 8). Static temperatures were computed using the Mach numbers and corrected total temperatures, and the local velocities were then calculated.

JET PLUME RESULTS

Data obtained from probe traverses taken 0.5 cm downstream of the nozzle exit for the 10.2 and 7.6 cm conical nozzles are shown in figures 14 to 18. Velocity profiles for the 10.2 cm conical nozzle (fig. 14) and the 7.6 cm conical nozzle (fig. 15) operating at ambient temperature and at pressure ratios from 1.4 to 2.5 show very flat velocity profiles across both nozzles with the exception of the PR = 2.5 case for the 7.6 cm nozzle, which indicates that the probe is in a region of shocks. The velocity computed from the probe data is, in all cases, within 1 percent of the value computed from the upstream measurements at the nozzle facility adapter (fig. 2).

The same type of velocity profile information is presented in figures 16(a) and (b) for the two circular nozzles operating at a nominal 815 K total temperature. The velocity profiles show an asymmetry for both nozzles. However, the peak flat value of the velocity profile is as close to the value calculated from the upstream measurements as was the case for the cold data. The velocity profile asymmetries shown in figures 16(a) and (b) are caused by the asymmetric total temperature profiles measured by the probe. This is illustrated in figure 17, where the measured total pressure and total temperature profiles for the PR = 1.76, T_t = 814 K case are shown for the 10.2 cm conical nozzle. The total pressure shows a very uniform profile, while the asymmetry of the total temperature profile is evident. This total temperature asymmetry is attributed to a thermal lag associated with the total temperature probe as it moves into the hot stream. A true variation of total temperature across the stream of the magnitude shown in figure 17 was ruled out as the possible cause of the asymmetry because the combustor was located upstream of the acoustic muffler whose baffled path acted as an excellent mixing device. This was corroborated by the seven total temperature readings measured across the stream at the nozzle adapter section (fig. 2), where only a variation of 19 K was measured, as well as by slow fall-off of the indicated temperature as the probe moved out of the jet. In figure 18 is presented the velocity profile data for the 10.2 cm diameter conical nozzle operated at ambient temperature with the flow straightening screen used in the RAE studies in place. For this case, the jet plume data indicates jet velocities of the order of 91 to 95 percent of the velocity calculated from the upstream measurements. In addition, there appeared to be a slight velocity deficiency near the centerline of the nozzle.

ACOUSTIC RESULTS

Acoustic data for 126 test conditions were taken on the three test nozzles. Because of space limitations, the complete OASPL and SPL spectral data are not presented; however, they are available upon request. All the SPL and OASPL data are presented on a lossless basis. Comparisons are

presented in this section among the OASPL and SPL data obtained in this study, using different microphone arrays, with cold static data obtained at the RAE 7.3 m wind tunnel and with a prediction procedure (ref. 7) developed using previously obtained data.

Effect of Microphone Array

A comparison of the OASPL directivity normalized for nozzle size and microphone distance obtained with the four microphone arrays used in this program is shown in figure 19 for the three nozzles operating at PR = 1.75 and T_T = 283 K. The data for the 10.2 cm conical nozzle (fig. 19(a)) appears to have less variation at any one angle than the data for the 7.6 cm conical nozzle (fig. 19(b)). The odd behavior of the 3 m and 7.01 m sideline arrays data at 110° may have been caused by a microphone problem. In all cases, including the 8-lobe nozzle (fig. 19(c)), all the OASPL data for any one nozzle are within ±1.5 dB between θ = 60° and θ = 140° from the inlet axis, the variation increasing at the shallower angles. Similar normalized OASPL data are presented in figure 20 for the three nozzles operating at elevated temperature, T_t = 815 K, and PR = 1.76. As in the cold flow case, all the data for any one nozzle are within ±1.5 dB between θ = 60° and 140° from the inlet axis, with the exception of the value at θ = 140° for the 8-lobe nozzle using the 4.57 polar boom array, which appears to be erroneous.

The results from figure 19 indicate a systematic lower value obtained from the 4.57 m polar centerline array at angles between 140° and 160°. This trend is not apparent in the hot data shown in figure 20, where the 7.01 m sideline array yield lower values at 160°. The data used for the comparisons shown in figures 19 and 20, even though typical, were selected at random, and erroneous conclusions may be drawn from looking at only a limited amount of data. For this reason statistical comparisons were made involving all the data acquired. These statistical comparisons, which will be discussed later, indicate that the data from the 4.57 m polar centerline array yielded the lowest mean values and the 3 m sideline array yielded the highest mean values, but these mean values were within less than 1.0 dB of each other.

Effect of Nozzle Shape

A comparison of the normalized OASPL directivity of the 8-lobe and the 7.6 m conical nozzles is shown in figure 21, for the data measured on the 3 m sideline, for a supersonic and a subsonic case having approximately the same jet velocity (360 and 385 mps, respectively). For the supersonic case, the 8-lobe nozzle has a 3 to 11 dB reduction in noise compared with the conical nozzle depending on the angle, with the larger reductions generally occurring in the rearward quadrant. In the subsonic case, the 8-lobe suppressor had only a trivial reduction relative to the conical nozzle at angles forward of 110° while maintaining the same level of noise reduction at the rearward angles as in the supersonic case. The high value of normalized OASPL for both nozzles in the forward quadrant for the supersonic case indicates the presence of dominant shock noise. Spectral comparisons between the conical and 8-lobe nozzles for the supersonic case are shown in figure 22(a). The 8-lobe nozzle reduces the low frequency noise signifi-

NASA
FORMAL
REPORT

cantly at the 150° angle compared with that for the conical nozzle, while having no effect at the high frequencies. Because the low frequency noise was very dominant at this angle for the conical nozzle, there is a resultant 10.8 dB reduction in the OASPL with the 8-lobe nozzle. At 90° with the 8-lobe nozzle there is also a significant reduction of low and middle frequency noise relative to the conical nozzle, including some screech tones at 2 and 4 kHz. The 8-lobe nozzle data show an increase in noise level compared with that for the conical nozzle at frequencies above 20 kHz, where shock noise from the lobe jets should be present. This combination yields an OASPL reduction of 3.4 dB at 90° for the 8-lobe nozzle relative to the conical nozzle.

The spectral comparison for the subsonic case is shown in figure 22(b). At both angles shown, 90° and 150°, the effect is similar to that for the supersonic case: the 8-lobe nozzle low frequency noise is appreciably reduced compared with the conical nozzle, but the high frequency noise is increased more than in the supersonic case shown in figure 22(a). As the conical nozzle high frequency noise is so much lower in level than the low frequency noise at the 150° angle, the OASPL reduction for the 8-lobe compared with the conical remains high (9.1 dB), even though the peak frequency shifts from 1.25 kHz for the conical to 6 kHz for the 8-lobe. At the 90° angle, however, the increase in high frequency noise for the 8-lobe nozzle is sufficient to negate the low frequency noise reduction, and the OASPL values for both nozzles are basically the same.

When these results are applied to nozzles suitable for engine use, perhaps 10 times larger in diameter, the noise reduction benefits of a nozzle such as the 8-lobe nozzle will be very much diminished because the frequency range where the noise level is lower for the 8-lobe nozzle will be below the audible range. It is even possible that the 8-lobe nozzle may have a larger perceived noise level in those cases because of the high frequency noise increase over that for the conical nozzle.

Comparison with Data from RAE Facility

The conical nozzle data acquired in this study are compared in this section with published static cold jet noise data from the RAE 7.3 m wind tunnel facility. The RAE acoustic data for the 7.6 cm nozzle (ref. 5) were taken on a 2.5 m sideline. The cold air flowed through a cascade bend and a screen flow straightener. The screen flow straightener is the same as that shown in figure 2 and used at NASA for a limited number of tests. In order to measure the flow, a reference pressure probe was located upstream of the cascade and calibrated with a total pressure pitot tube measurement at the nozzle exit. The 10.2 cm nozzle acoustic data (ref. 6) were measured on a 2.17 m sideline. The cold air supply line was the same as that in reference 5. The pressure measurement location was also the same as that in reference 5, but in this case, the reference pressure probe was calibrated against a 9-point pitot rake at the exit plane. A comparison of the RAE normalized OASPL data for the two conical nozzles indicates a nominal 5 to 7 dB difference between these nozzles, with the higher normalized OASPL values being measured with the 10.2 cm diameter nozzle. A possible reason for this discrepancy will be discussed later.

The OASPL data from two cold flow test conditions at the NASA-Lewis facility normalized for measuring distance are compared in figure 23 with results obtained at the Royal Aircraft Establishment 7.3 m free-jet tunnel

for the 10.2 cm diameter nozzle at two jet velocities. The data from the two facilities agree reasonably well, being within 1.5 dB at all angles between 90° and 145°.

A more general type of comparison with the 10.2 cm data from RAE is shown in figure 24, where results from 8 NASA Lewis tests using the four different microphone arrays and both the 10.2 and 7.6 cm nozzles are compared to the RAE directivity data. On this basis, the RAE data for the 10.2 cm nozzle falls in the middle of the NASA-Lewis data band. The RAE data for the 7.6 cm conical nozzle as reported in reference 5 is about 5 dB quieter on a normalized basis. A possible reason for this disagreement may be that the calibration of the flow for the 7.6 cm conical nozzle at RAE was performed without the screen and the screen subsequently used for the acoustic tests. Further evidence to support this viewpoint is given in figure 25 where the normalized RAE OASPL data for the 7.6 cm diameter conical nozzle are compared with the data taken in this study for the 10.2 cm nozzle with the straightening screen installed. The agreement between the 7.6 cm data from RAE and the NASA data with the screen is very good even though the actual velocity for the NASA tests with the screen is known to be much lower than the nominal value calculated from the upstream conditions (see fig. 18). Figure 25 also shows the 10.2 cm nozzle RAE data as a dotted curve to point out the difference between the two sets of RAE data when compared on a normalized basis.

A spectral comparison is shown in figure 26 where normalized SPL data at 90° are plotted as a function of Strouhal number for several cases: the RAE 7.6 cm diameter conical data, the NASA data for the 7.6 and 10.2 cm diameter conical nozzles without screen and the NASA data for the 10.2 cm conical nozzle with screen. As was the case for the normalized OASPL comparison, the shape and level of the RAE 7.6 cm conical data agree very well with the 10.2 cm diameter data with screen (which has an erroneous jet velocity). The agreement between the NASA 7.6 and 10.2 cm conical data without screen is good, but again the shape and level differ from the RAE 7.6 cm nozzle. For this comparison the jet velocity calculated from upstream measurements was used in all cases.

Comparison of Data with a Prediction Procedure

The SPL spectral and OASPL directivity data obtained herein are now compared with the predicted values from the procedure developed in reference 7. The spectral data for the 10.2 cm diameter conical nozzle at the 3 m sideline at all temperatures and pressures are compared with two different prediction procedures in figures 27(a) to (h). Comparisons are made at four angles (60°, 90°, 130°, and 150°) for all four pressure ratios and both temperature levels. The dual predicted values result from different assumptions made with regard to source distribution along the jet axis: one method assumes all noise sources concentrated at the nozzle exit plane; the other assumes the noise sources to be distributed along the jet axis. The second approach, as suggested in reference 7, is a better approximation insofar as it assumes the location to be a point source located at a distance X_θ downstream of the exit plane, this distance being independent of frequency and only a function of the angular position of the observer with respect to the nozzle exit. The prediction procedure, developed independently of the data taken in this program, predicts the peak noise frequency, level and the spectral shape around the peak frequency well except

when shock noise, which is not included in the prediction, becomes important. However, at very high frequencies, above 8 kHz, even when jet mixing noise is dominant, the agreement is not as good. Even though the use of the distributed source location approximation does not improve the agreement significantly, the general trend is in the right direction, especially in the high frequency range at the rearmost angles.

Comparisons of spectral data for the various micropnone arrays with predictions for the 10.2 cm conical nozzle at a 1.75 pressure ratio at cold and hot operating temperatures, assuming all noise sources at the exit plane, are shown in figures 28 and 29. The cold spectral data are shown in figure 28 at two angles: 90° and 140°. The agreement with the prediction does not change significantly regardless of the microphone array used. This also applies to the agreement between the hot data for the different arrays and the prediction as shown in figure 29.

In figure 30 some spectral comparisons for the 7.6 cm conical nozzle are presented. The type of general agreement is similar to that encountered with the 10.2 cm conical nozzle except perhaps at the 130° angle for the PR = 1.75, hot flow case (fig. 30(c)), where there is a large disagreement near the peak value.

The data obtained at PR = 1.74 for the 10.2 cm conical nozzle with the flow screen installed are compared with prediction values in figure 31 at angles of 90° and 150°. For this case, the agreement with the prediction at the jet velocity calculated from upstream conditions is very much different than for the cases without the flow screen; the predicted values are higher than the measured values by 3 to 4 dB throughout the spectrum. When compared with the prediction at the velocity values measured at the exit plane of the nozzle using the traversing probe (fig. 18) the agreement is better (within 2 dB).

The above spectral comparisons with the prediction procedure represent only sample cases. More complete comparisons have been made for the values of OASPL. The OASPL values for all the subsonic data taken with the 10.2 and 7.6 cm conical nozzles without the flow screen installed are compared with the prediction of reference 7 assuming a distributed source location along the jet axis in figures 32 and 33. In figure 32 are shown the hot and cold flow data at a PR = 1.4 while in figure 33 are shown the data at a PR = 1.75. The comparison was made by calculating the OASPL* value for each condition. This value is defined as follows:

$$\mathrm{OASPL}^* = \mathrm{OASPL} - 10 \log \frac{A}{R^2} - 10 \log \left(\frac{\rho_j}{\rho_o}\right)^{\omega} - 10 \log \left(\frac{V_j}{c_o}\right)^{7.5} + 15 \log\left[(1 + M_c \cos \theta)^2 + \alpha^2 M_c^2\right] \qquad (1)$$

OASPL* should have a constant value of 141 for all angles and operating conditions according to reference 7.

The comparison shown in figure 32 for a PR = 1.4 shows most of the data falling within 2 dB of the 141 value. Both the data for the 10.2 cm conical nozzle (fig. 32(a)) and the 7.6 cm nozzle (fig. 32(b)) indicate that the results from the high temperature jet are higher than these for the cold jet. The discrepancies encountered with the data are greater at the rear angles near the jet axis. The results for PR = 1.75 shown in figures 33(a) and (b) for the 10.2 cm and 7.6 cm diameter nozzles, respectively, show

basically the same trends, the discrepancy being the greatest at the 160° angle for the hot jet data. The separation between hot and cold data implies that the temperature effects incorporated in the prediction procedure as a density correction perhaps could be modified to bring about a better agreement between hot and cold data.

Statistical Data Comparison

As previously indicated under the discussion of the effect of microphone arrays, a statistical comparison has been made in order to compare all the data obtained, rather than depend on observations based on small samplings of the data. In order to compare all the data on a consistent basis, the differences between the measured values of OASPL and the predicted values calculated from the procedure of reference 7 were calculated. This prediction procedure was used as the yard stick because it had been previously substantiated by comparison with recent data from the Lockheed Corporation anechoic chamber (ref. 12).

The mean value of the difference between experimental and calculated values (Δ_{mean}) is a measure of goodness of the prediction procedure for a data set. The standard deviation is a measure of the repeatability of the data when the proper grouping is compared.

Table 1 is a summary of the OASPL difference mean values and standard deviations when grouped by different categories. The first grouping consists of all the subsonic data obtained without using the internal flow straightening screen. For these 61 test runs, the mean value of the difference between experimental and calculated values of OASPL for all the angles is 0.8 dB with a standard deviation of 1.8 dB. The distribution among the different angles varies. The larger mean differences from the predicted values occur at 130° and 140° (1.6 and 1.9 dB) while the largest standard deviations occur at 160° (2.4 dB). The prediction procedure throughout the arc under-predicts the OASPL values ($\Delta_{mean} > 0$) except at 110° and 160° (where $\Delta < 0$). The mean difference of 0.8 dB with a standard deviation of 1.8 dB compares with the mean difference of 0.1 dB and standard deviation of 1.6 dB observed for the data of reference 12 over a much smaller sampling of data.

The next two groupings divide the subsonic data into cold (290 K) and hot (811 K) flow data. The cold flow data agree better with the prediction procedure and have a lower standard deviation than the hot flow data. The next four groups in table 2 compare the statistics of the subsonic data among the difference microphone arrays used to measure the data. Examination of the Δ_{mean} and standard deviations among these four groupings show the 4.57 m polar centerline array yielded the lowest Δ_{mean} values while the 3.00 m sideline array yielded the highest Δ_{mean} values, but these Δ_{mean} values were within less than 1.0 dB of each other. The standard deviations are about the same. When the data are divided into the two subsonic pressure ratios tested (1.4 and 1.75) in groups 8 and 9, no trend whatsoever is obtained.

SUMMARY OF RESULTS

Static acoustic data have been obtained at the NASA-Lewis Research Center outdoor jet noise facility with a 10.2 cm diameter conical nozzle, a

7.6 cm diameter conical nozzle and a 7.6 cm equivalent diameter 8-lobe nozzle, using four different microphone arrays. The nozzles tested had been previously tested at other facilities including the Royal Aircraft Establishment (RAE) 7.3 m wind tunnel. The four microphone arrays consisted of a 3.00 m sideline microphone array and a 7.01 m sideline microphone array, both using centerline and ground microphones to cover the spectral field up to 80 kHz; a 4.57 m polar array mounted in the vertical plane of the nozzle axis and a 4.57 m polar array set in the horizontal centerline plane of the nozzle axis. On the basis of the present study, the acoustic results obtained can be summarized as follows:

1. No appreciable difference was found among the results obtained from the four microphone arrays.

2. The data for the 10.2 cm conical nozzle agreed with the data obtained at the RAE 7.3 m wind tunnel.

3. The data for the 7.6 m conical nozzle did not agree with the data obtained at the RAE 7.3 m wind tunnel. However, as the 7.6 and 10.2 cm data from the NASA-Lewis facility agreed with each other when normalized for size it is concluded that the RAE data has an apparent discrepancy. Data taken at NASA Lewis Research Center on the 10.2 cm conical nozzle with an internal flow straightening screen, which reduced the exit velocity relative to the velocity calculated from upstream measurements, agreed with the RAE 7.6 cm diameter nozzle data when normalized for size.

4. The 10.2 and 7.6 cm conical nozzle acoustic data were compared with the predictions from a NASA developed procedure. The spectral comparison with the jet mixing noise data shows good agreement with the frequency at which peak noise occurs as well as with the spectral shape near the peak noise range.

5. A statistic analysis of the OASPL differences between experimental and predicted values show a mean difference of 0.8 dB over all the angles, with a standard deviation of 1.8 dB. The prediction procedure agrees slightly better with the cold than with the hot data; however, there are no noticeable effects of microphone array or operating pressure.

6. The 8-lobe nozzle gave OASPL reductions relative to the conical nozzle. These reductions ranged from 11 dB at the rearward angles to 3 dB at angles from 30° to 90° for the supersonic case. There was no reduction in OASPL at the forward angles for the subsonic cases, even though the same reduction as for the supersonic case was maintained at the rearward angles.

REFERENCES

1. U. Von Glahn and D. Groesbeck, "Noise of Deflectors Used for Flow Attachment with STOL-OTW Configurations," NASA TM-73809 (December 1977).

2. W. A. Olsen and R. Friedman, "Jet Noise from Coaxial Nozzles over a Wide Range of Geometric and Flow Parameters," AIAA Paper No. 74-43 (January 1974).

3. J. H. Goodykoontz and J. R. Stone, "Experimental Study of Coaxial Nozzle Exhaust Noise," AIAA Paper No. 79-0631 (March 1979).

4. J. R. Stone, J. H. Goodykoontz, and O. A. Gutierrez, "Effects of Geometric and Flow-Field Variables on Inverted-Velocity-Profile Coaxial Jet Noise and Source Distribution," AIAA Paper No. 79-0635 (March 1979).

5. J. B. W. Edwards, "Comparative Measurement of the Noise of Cold Air Jets from Three Nozzles under Static and Forward - Speed Conditions," RAE-TM-Aero-1692, Royal Aeronautical Establishment, Benford, England, 22 Sept. 1976.

6. B. J. Cocking and W. D. Bryce, "An Investigation of the Noise of Cold Air Jets Under Simulated Flight Conditions," Rep. No. R-334 (September 1974).

7. J. R. Stone and F. J. Montegani, "An Improved Prediction Method for the Noise Generated in Flight by Circular Jets," NASA TM-81470 (April 1980).

8. G. E. Glawe, F. S. Simmons, and T. M. Stickney, "Radiation and Recovery Corrections and Time Constants of Several Chromel-Alumel Thermocouple Probes in High-Temperature, High-Velocity Gas Streams," NACA TN-3766 (1956).

9. W. L. Howes, "Ground Reflection of Jet Noise," NASA TR R-35 (1959).

10. F. D. Shields and H. E. Bass, "Atmospheric Absorption of High Frequency Noise and Application to Fractional Octave Bands," NASA CR-2760 (1977).

11. "Equations, Tables, and Charts for Compressible Flow," NACA Rep. 1135 (1953).

12. H. K. Tanna, P. D. Dean, and R. H. Durrin, "The Generation and Radiation of Supersonic Jet Noise, Vol. III, Turbulent Mixing Noise Data," LG76ER0133-Vol-3, Lockheed-Georgia Co., Marietta, GA (June 1976). (AD-A032882, ARAPL-TR-76-65-Vol-3).

TABLE 1. - SUMMARY OF MEAN VALUE AND STANDARD DEVIATIONS FOR DIFFERENCES BETWEEN EXPERIMENTAL AND CALCULATED VALUES OF OASPL FOR VARIOUS GROUPINGS OF DATA

Type of data	No. of test conditions		Range from inlet axis, deg									Overall
			30	40	60	90	110	130	140	150	160	
1 - All subsonic data	61	Δ_{mean}	1.2	1.4	1.3	0.6	-0.3	1.6	1.9	0.7	-0.3	0.8
		ST. DEV.	1.4	1.3	.8	.9	1.4	2.0	1.4	2.0	2.4	1.8
2 - Cold subsonic data	33	Δ_{mean}	1.4	1.4	1.2	0.0	-1.2	0.5	0.8	0.4	1.3	0.6
		ST. DEV.	1.2	1.4	.8	.7	1.2	1.0	.8	2.4	1.3	1.5
3 - Hot subsonic data	28	Δ_{mean}	0.9	1.5	1.4	1.3	0.6	3.0	3.3	1.1	-2.3	1.1
		ST. DEV.	1.6	1.2	.8	.7	1.0	2.0	.6	1.2	1.9	2.0
4 - Subsonic data measured at 3 m sideline	14	Δ_{mean}	1.6	---	1.6	1.4	-0.7	1.8	2.0	1.8	0.7	1.3
		ST. DEV.	.7	---	.5	.8	.8	1.8	1.3	.5	2.0	1.5
5 - Subsonic data measured at 7.01 m sideline	17	Δ_{mean}	---	1.4	1.2	0.3	-1.2	2.7	2.2	1.5	-0.3	1.0
		ST. DEV.		1.3	.9	.8	1.8	2.1	1.1	1.0	3.2	2.1
6 - Subsonic data measured at 4.57 m polar boom	12	Δ_{mean}	2.2	---	1.5	0.5	0.3	---	2.3	-1.2	-0.6	0.7
		ST. DEV.	.8	---	.6	.6	1.1	---	1.5	3.3	1.9	2.1
7 - Subsonic data measured at 4.57 m polar, centerline	18	Δ_{mean}	0.1	---	1.1	0.3	0.3	0.4	1.3	0.3	-1.0	0.4
		ST. DEV.	1.4	---	1.0	1.0	1.0	1.2	1.5	1.0	1.6	1.4
8 - All data at PR = 1.4	21	Δ_{mean}	0.1	1.0	0.9	0.4	-0.2	1.7	2.0	1.0	0.8	0.9
		ST. DEV.	1.4	1.0	.9	1.0	1.3	2.0	1.5	2.3	1.7	1.7
9 - All data at PR = 1.75	40		1.7	1.7	1.5	0.7	-0.4	1.5	1.9	0.5	-0.9	0.8
		ST. DEV.	1.0	1.4	.7	.9	1.5	2.0	1.4	1.8	2.4	1.8

$\Delta = OASPL_{exp} - OASPL_{calc}$.
$OASPL_{calc}$ from prediction procedure, ref. 7.
Values of Δ_{mean} and St. Deviations in dB.

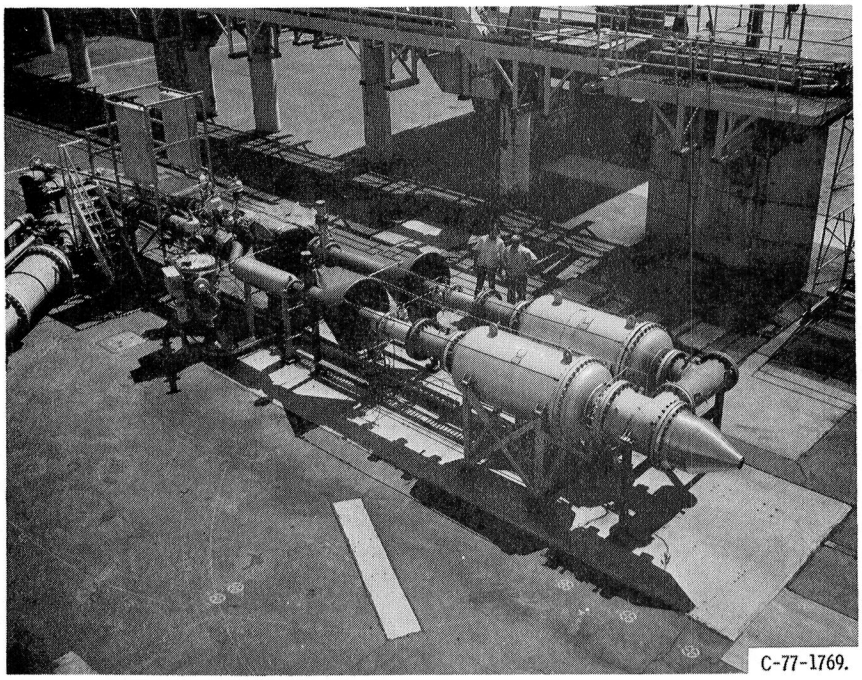

Figure 1. - NASA-Lewis outdoor jet acoustic facility.

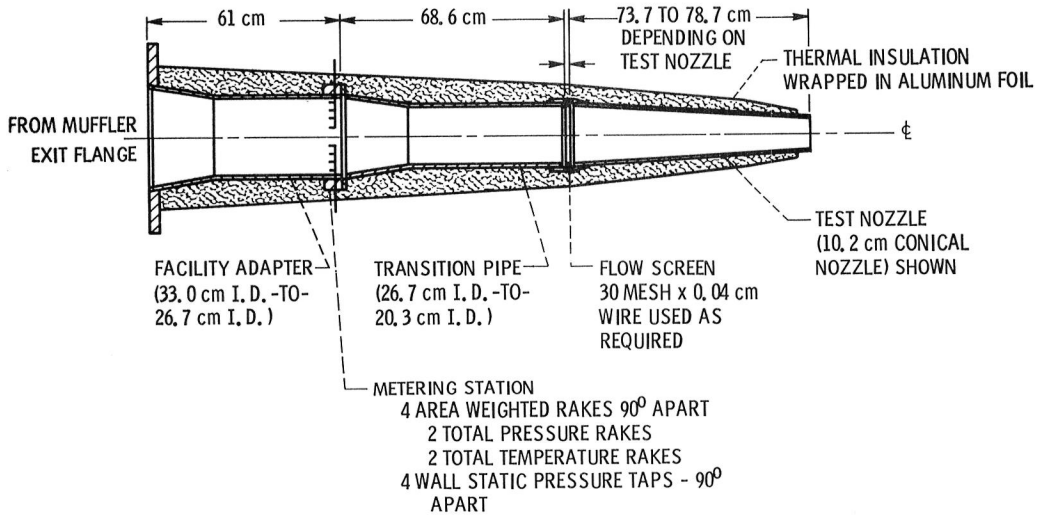

Figure 2. - Installation of facility adapters and test nozzles.

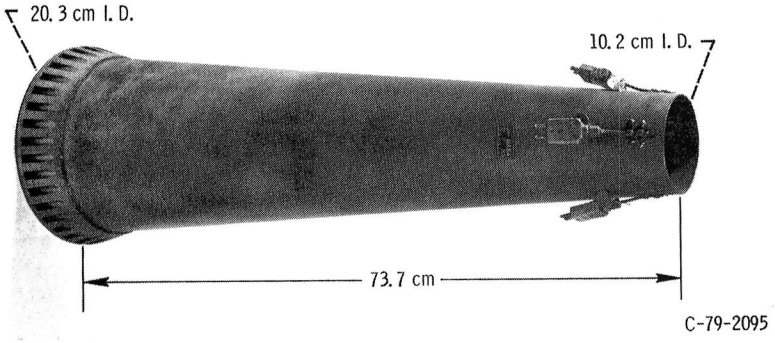

Figure 3. - 10.2 cm diameter conical nozzle.

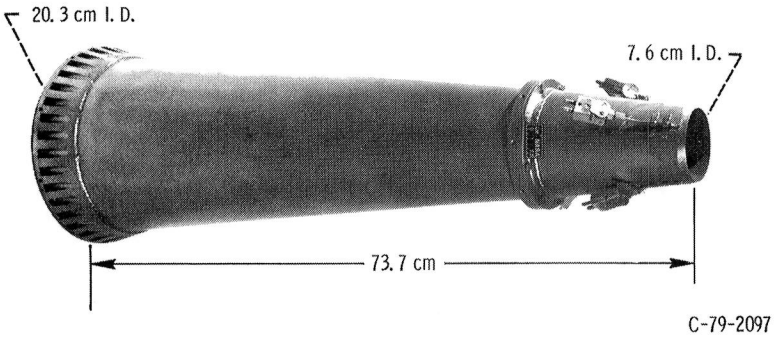

Figure 4. - 7.6 cm diameter conical nozzle.

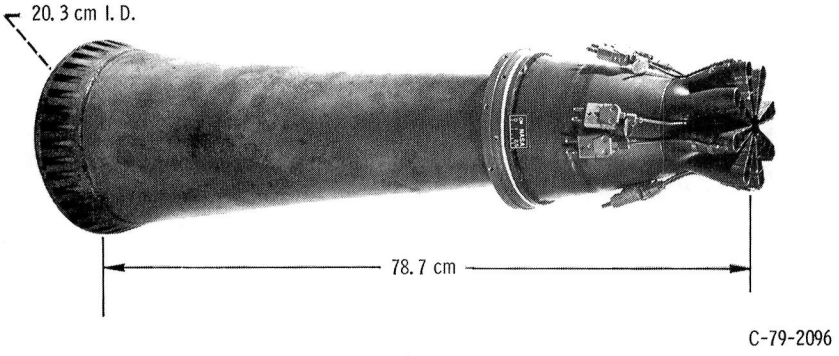

Figure 5. - 8-Lobe nozzle 7.6 cm equivalent diameter.

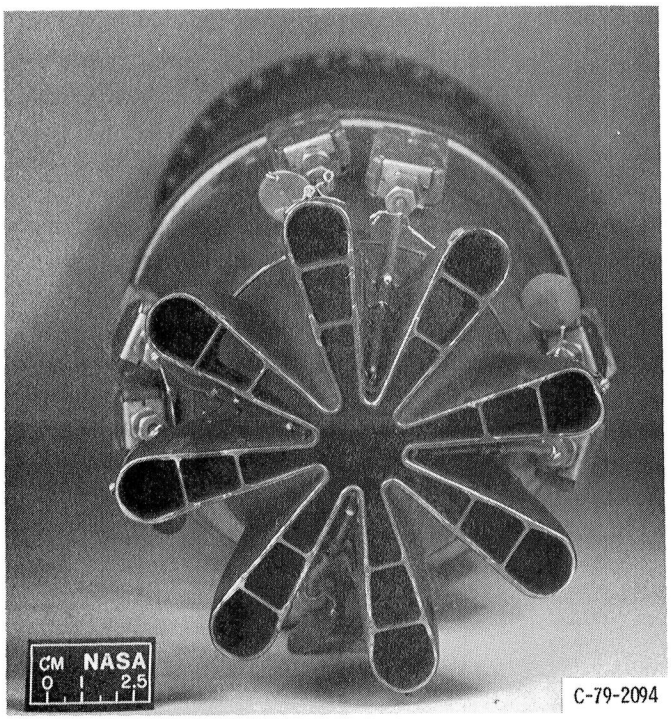

Figure 6. - End view of 8-lobe nozzle.

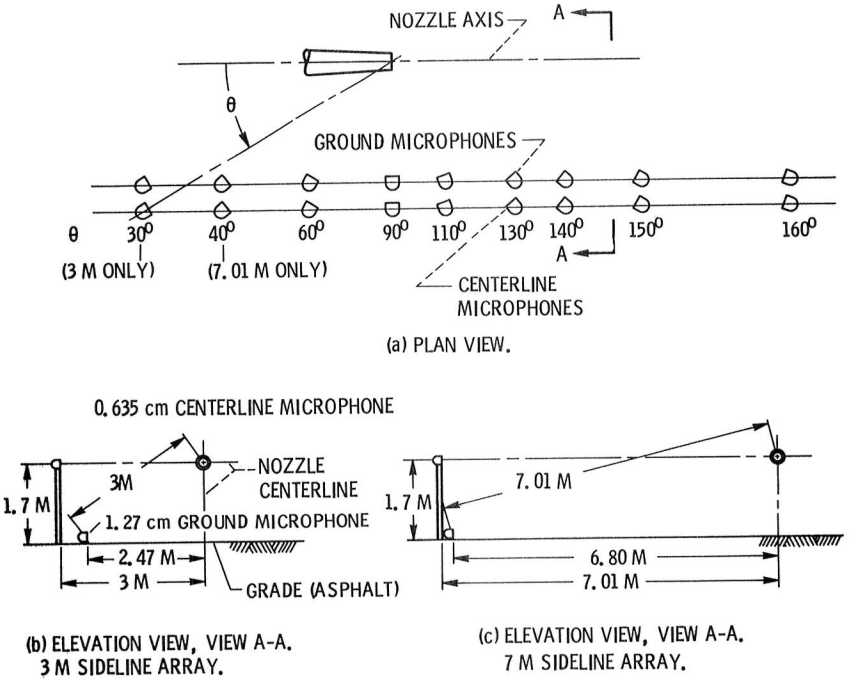

Figure 7. - 3 meter and 7.01 meter sideline microphone layouts.

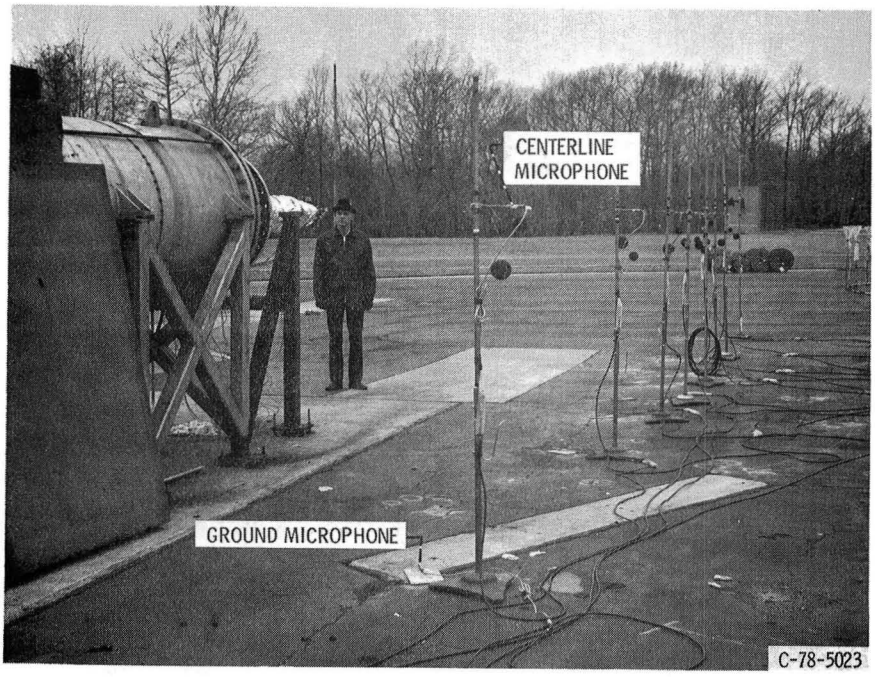

Figure 8. - View of acoustic arena showing 3 m sideline microphone array.

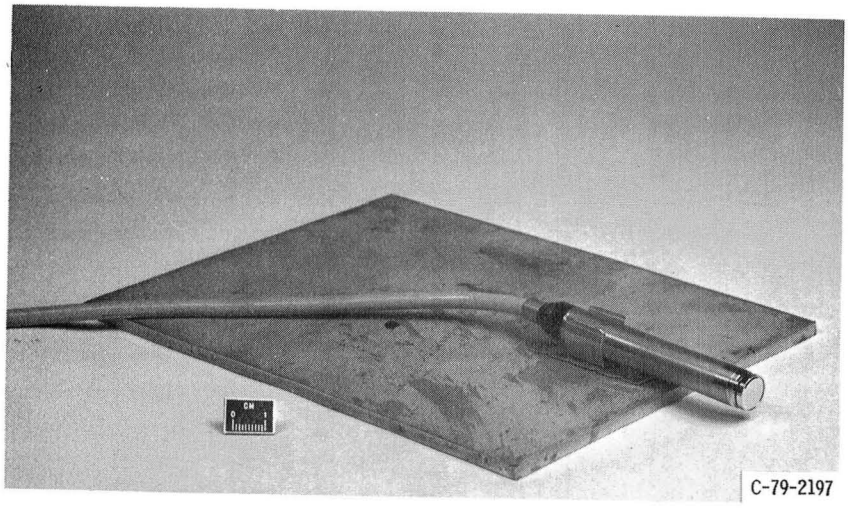

Figure 9. - Mounting of 1.27 cm ground microphones.

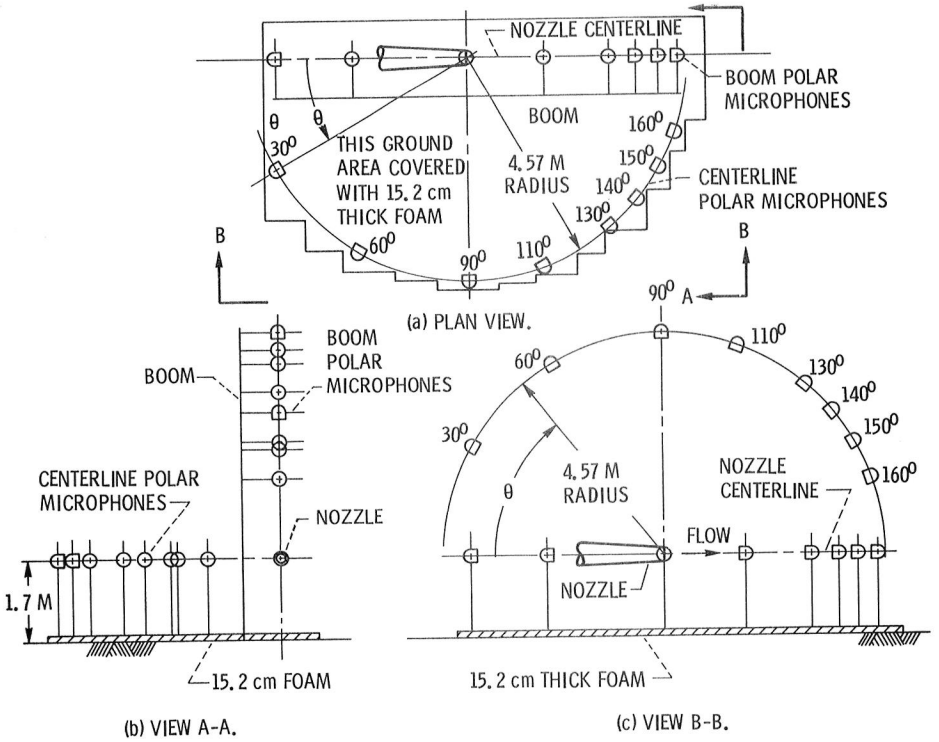

Figure 10. - Boom and centerline polar microphone layouts. 0.635 cm microphones.

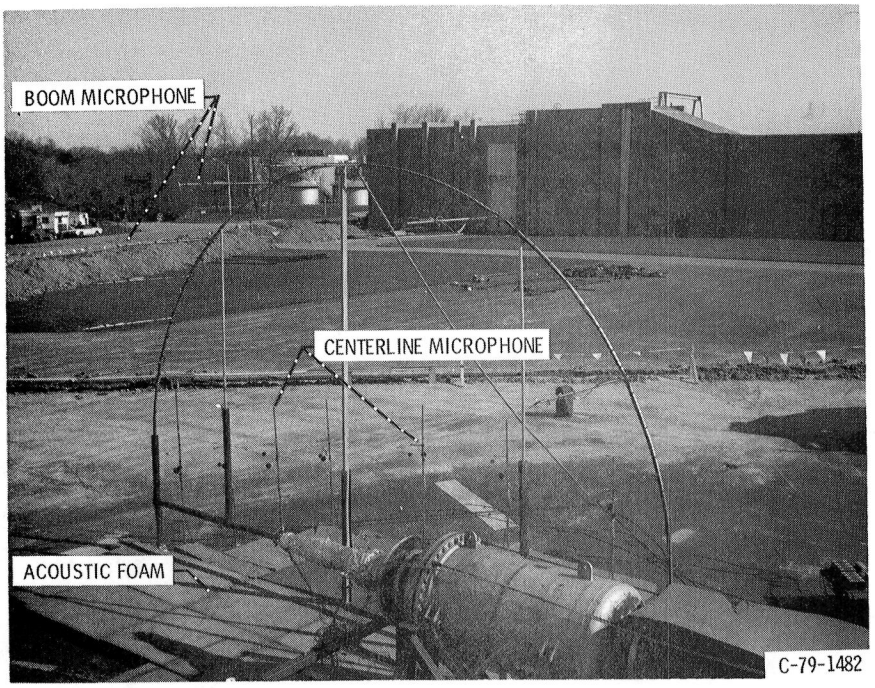

Figure 11. - View of acoustic arena showing 4.57 M polar boom and 4.57 M polar centerline arrays.

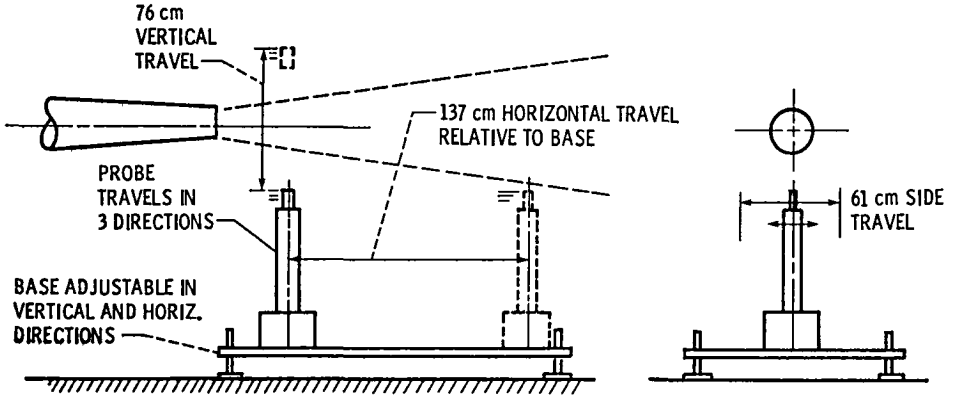

Figure 12. - Jet plume survey arrangement.

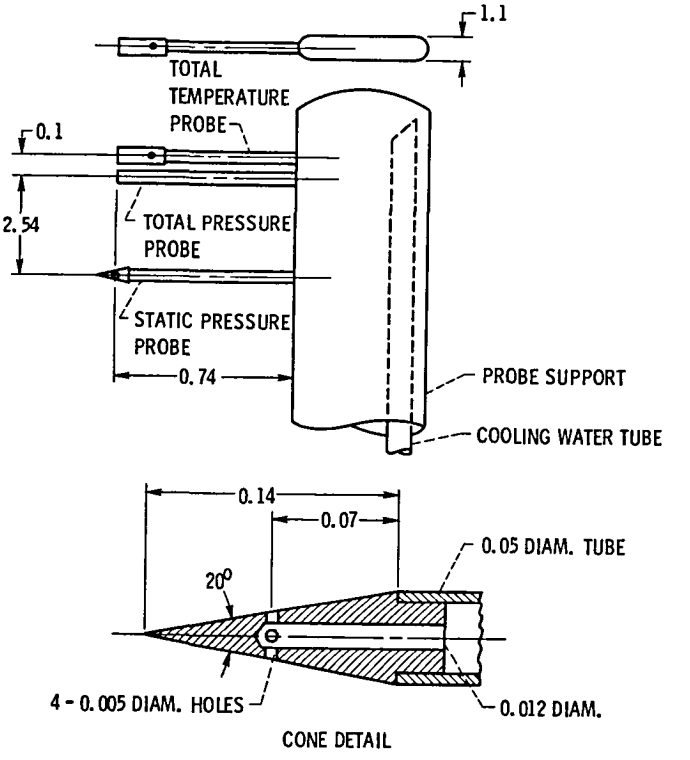

Figure 13. - Jet exhaust plume probe (all dimensions in centimeters).

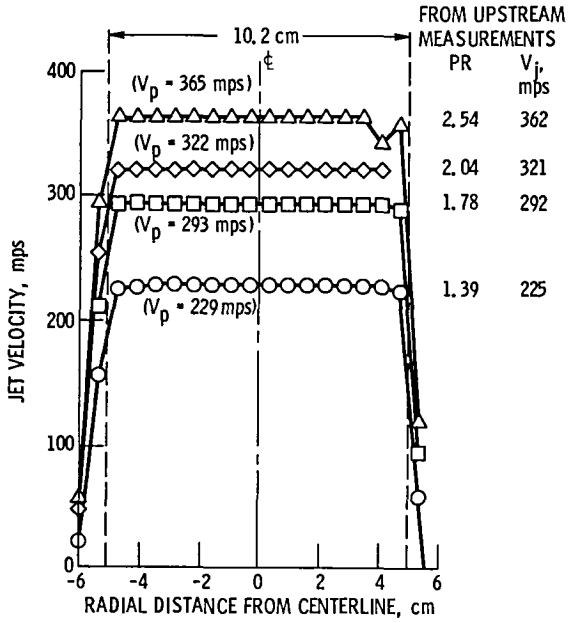

Figure 14. - Velocity profiles, 0.5 cm downstream of exit for 10.2 cm conical nozzle without screen. Ambient jet temperature.

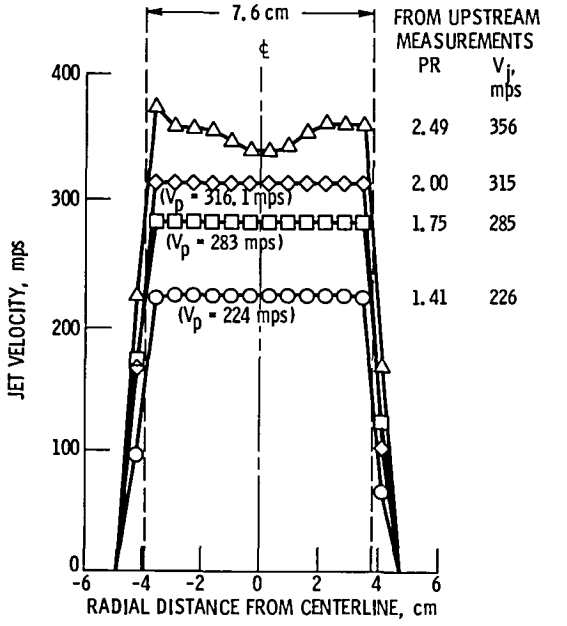

Figure 15. - Velocity profiles, 0.5 cm downstream of exit for 7.6 cm conical nozzle without screen. Ambient jet temperature.

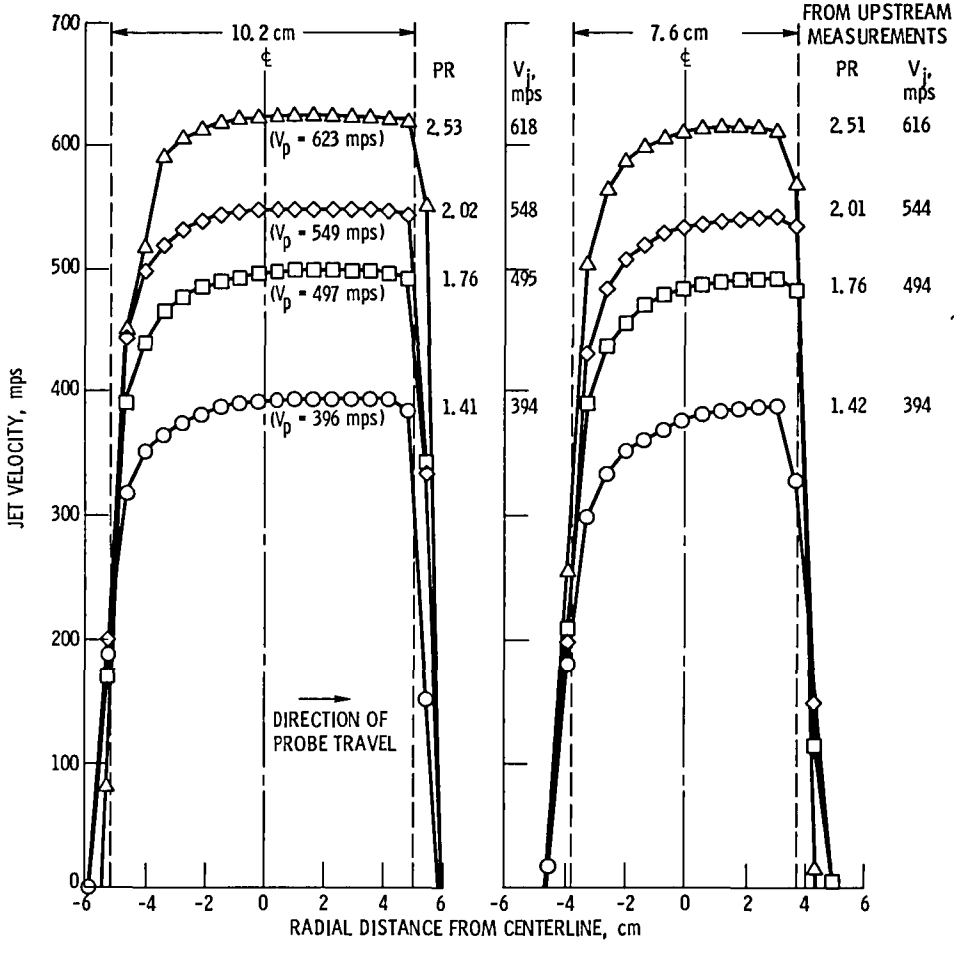

(a) 10.2 cm DIAMETER NOZZLE. (b) 7.6 cm CONICAL NOZZLE.

Figure 16. - Velocity profiles, 0.5 cm downstream of exit for conical nozzles without screen. Nominal jet total temperature, 815 K.

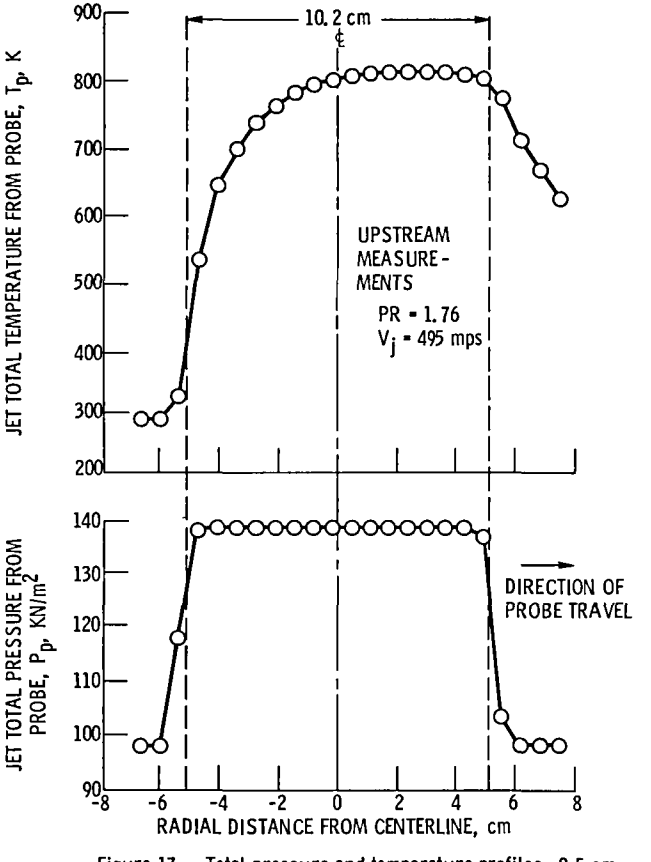

Figure 17. - Total pressure and temperature profiles, 0.5 cm downstream of exit for 10.2 cm diameter nozzle without screen.

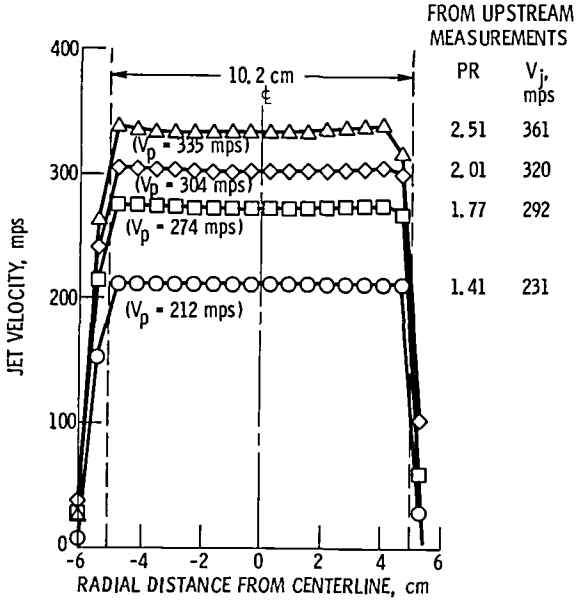

Figure 18. - Velocity profiles 0.5 downstream of exit for 10.2 cm conical nozzle with screen. Ambient jet temperature.

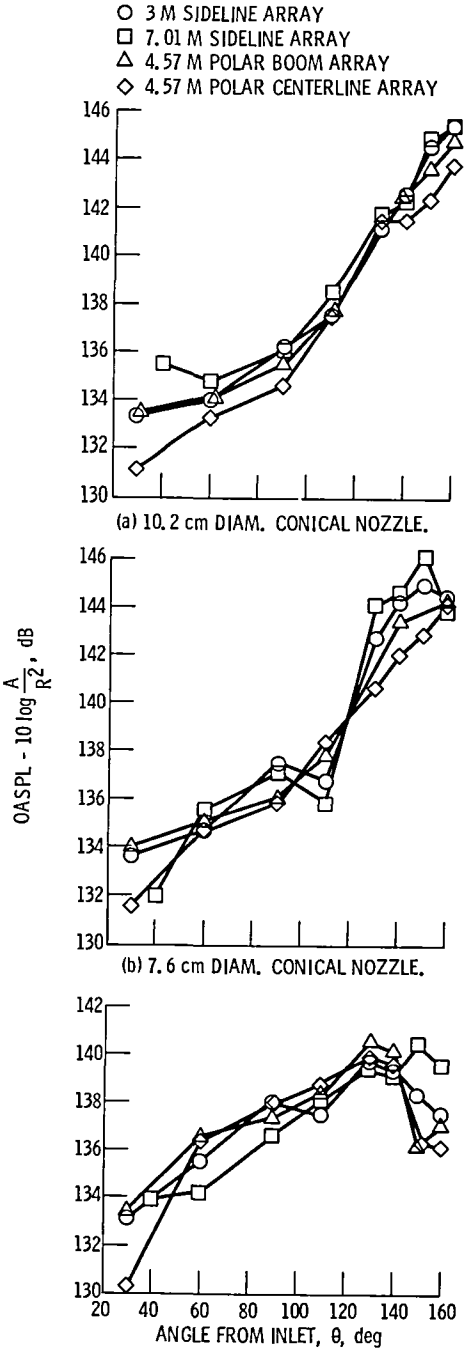

Figure 19. - Effect of microphone array on measured cold-flow OASPL directivity. Nominal conditions: V_j, 293 mps; T_T, 283 K; PR, 1.75.

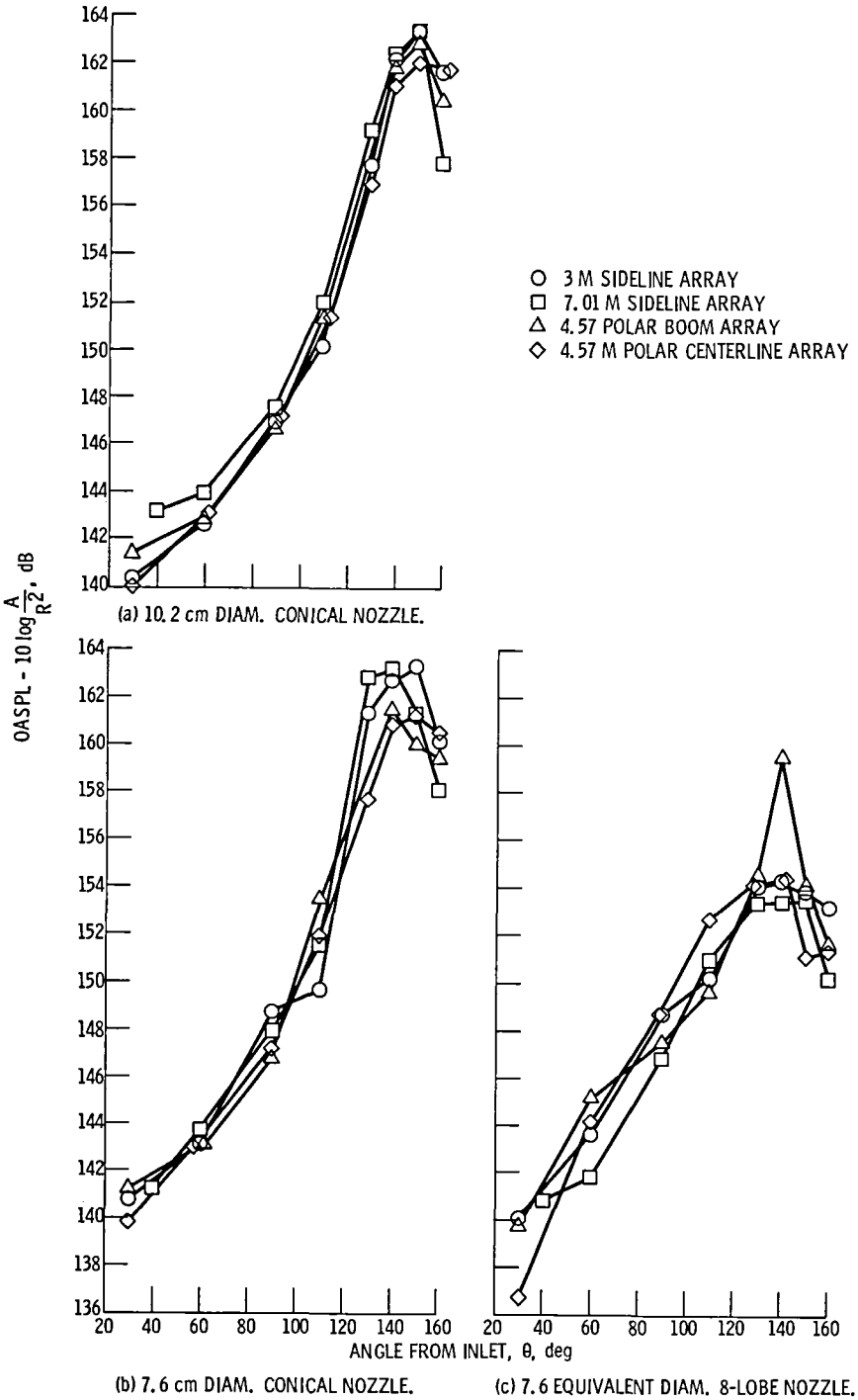

(a) 10.2 cm DIAM. CONICAL NOZZLE.

(b) 7.6 cm DIAM. CONICAL NOZZLE.

(c) 7.6 EQUIVALENT DIAM. 8-LOBE NOZZLE.

Figure 20. - Effect of microphone array on measured hot-flow OASPL directivity. Nominal conditions: V_j, 495 mps; T_T, 815 K; PR, 1.75.

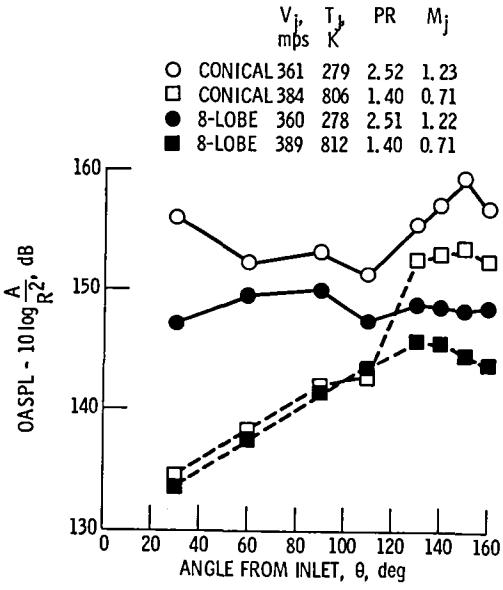

Figure 21. - Comparison of OASPL directivity for the 7.6-cm diameter conical nozzle and the 8-lobe nozzle. 3 M sideline.

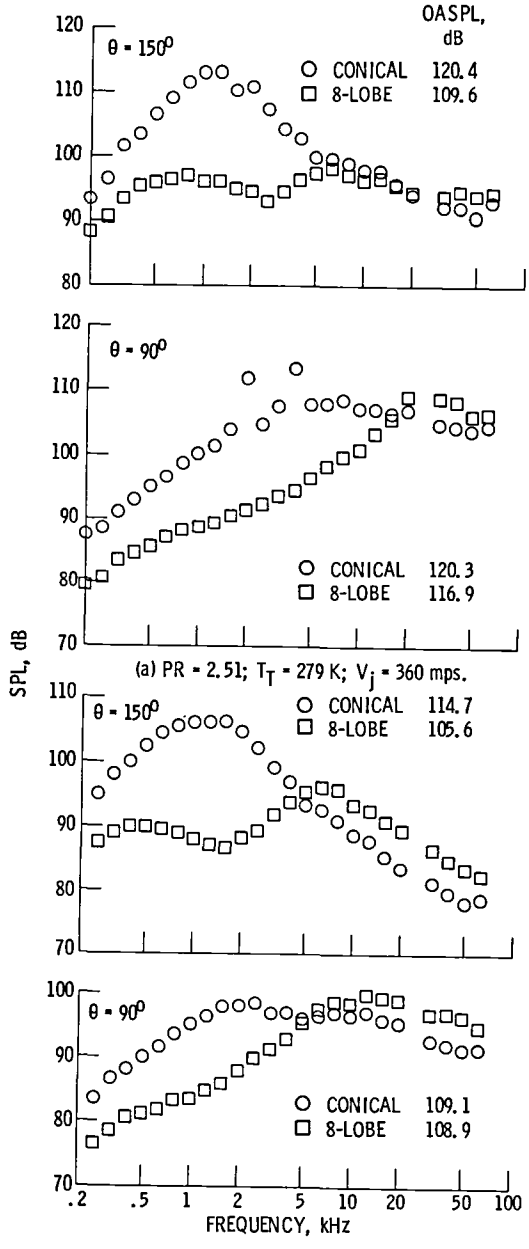

(a) PR = 2.51; T_T = 279 K; V_j = 360 mps.

(b) PR = 1.40; T_T = 809 K; V_j = 387 mps.

Figure 22. - Comparison of jet noise spectra for a 7.6 cm conical nozzle and an 8-lobe nozzle.

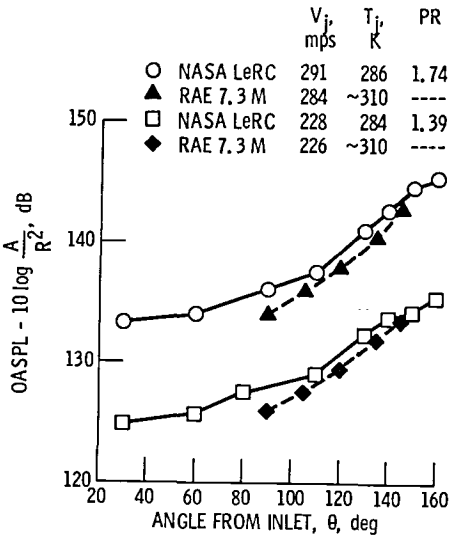

Figure 23. - Comparison of NASA and RAE normalized OASPL directivities for a 10.2 cm conical nozzle.

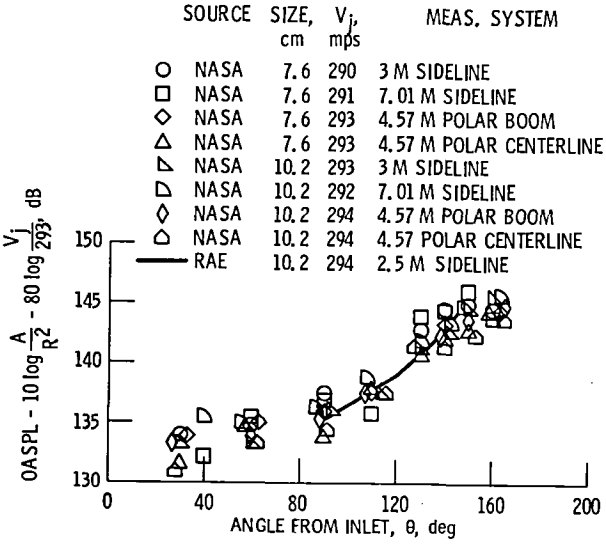

Figure 24. - Comparison of normalized OASPL directivities for 7.6 and 10.2 cm conical nozzles at NASA and the 10.2 cm nozzle at RAE. Nominal ambient jet temperature.

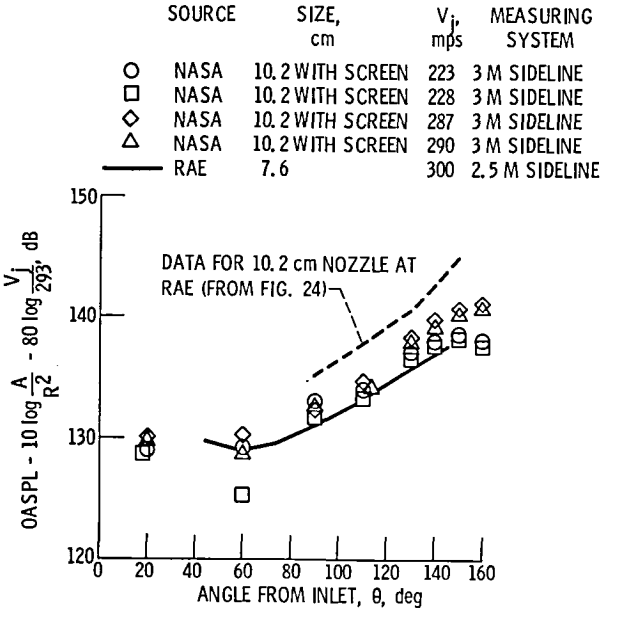

Figure 25. - Comparison of OASPL directivity for 7.6 cm conical nozzle at RAE and 10.2 cm conical nozzle at NASA facilities using flow screen. Ambient jet temperature.

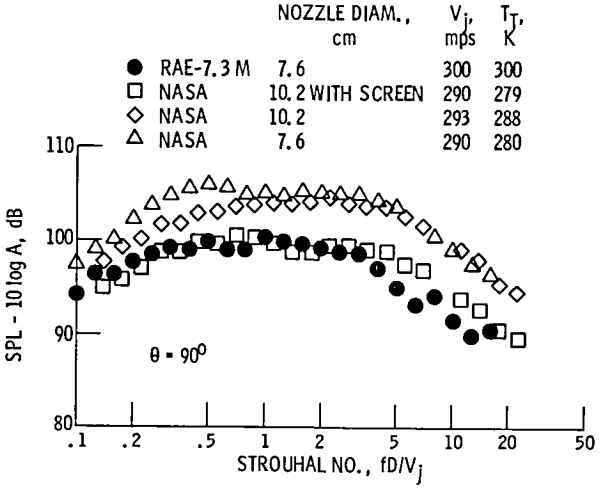

Figure 26. - Comparison of normalized SPL as a function of Strouhal number between NASA data and 7.6 cm diameter conical nozzle RAE data.

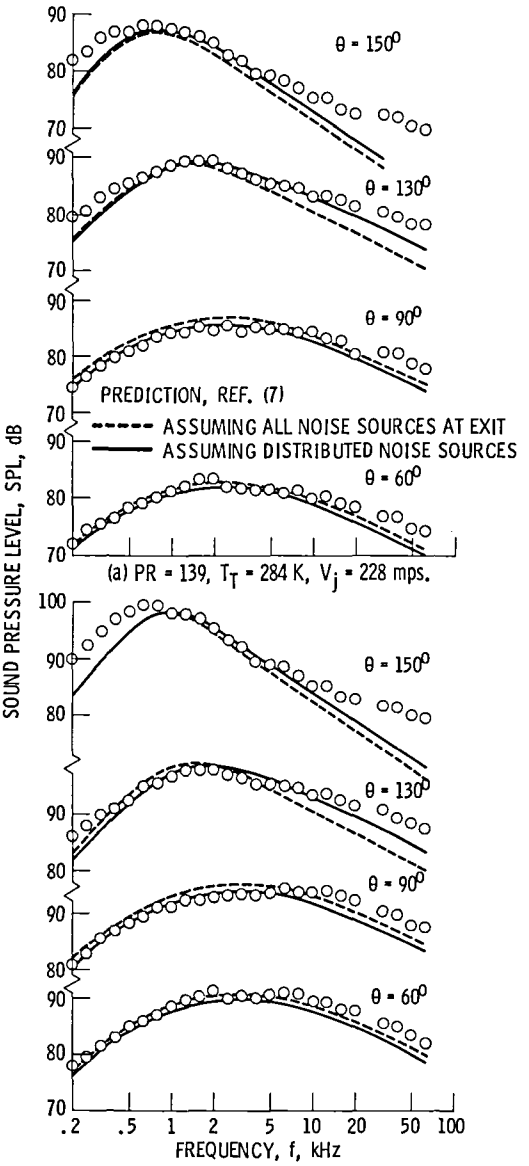

(a) PR = 139, T_T = 284 K, V_j = 228 mps.

(b) PR = 1.74, T_T = 288 K, V_j = 293 mps.

Figure 27. - Comparison of 10.2 cm conical nozzle spectral data with prediction. 3-M sideline.

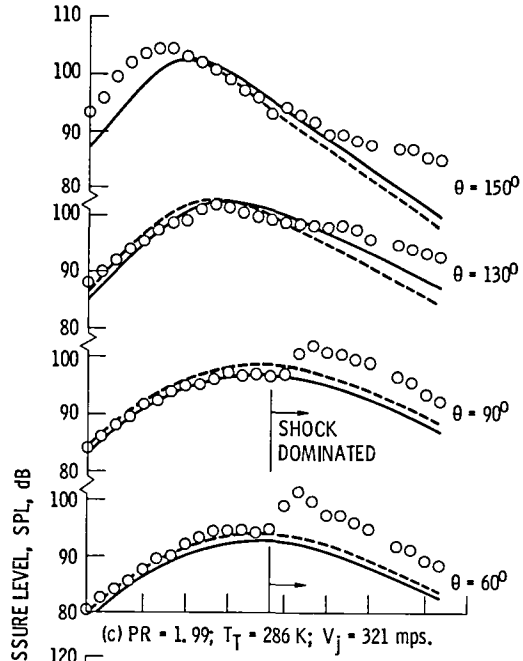

(c) PR = 1.99; T_T = 286 K; V_j = 321 mps.

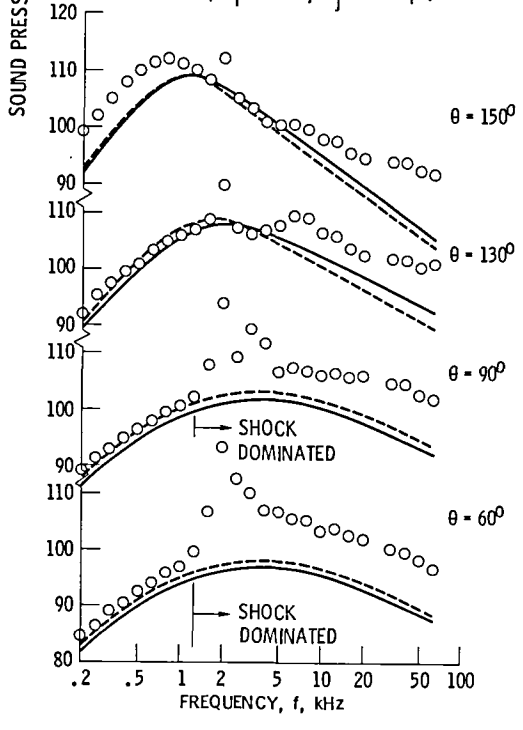

(d) PR = 2.49; T_T = 286 K; V_j = 364 mps.

Figure 27. - Continued.

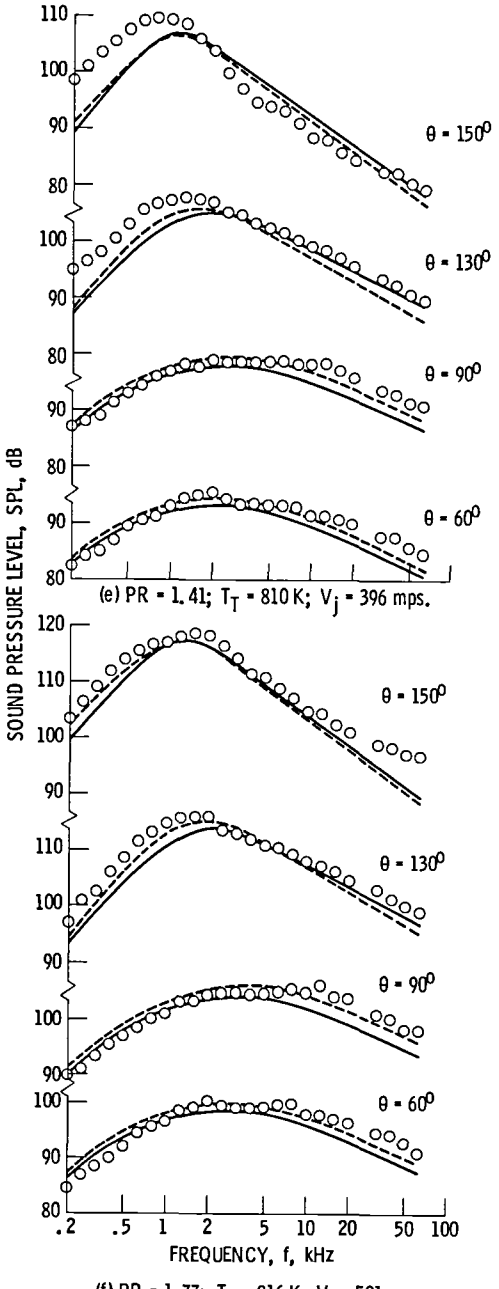

(e) PR = 1.41; T_T = 810 K; V_j = 396 mps.

(f) PR = 1.77; T_T = 816 K; V_j = 501 mps.

Figure 27. - Continued.

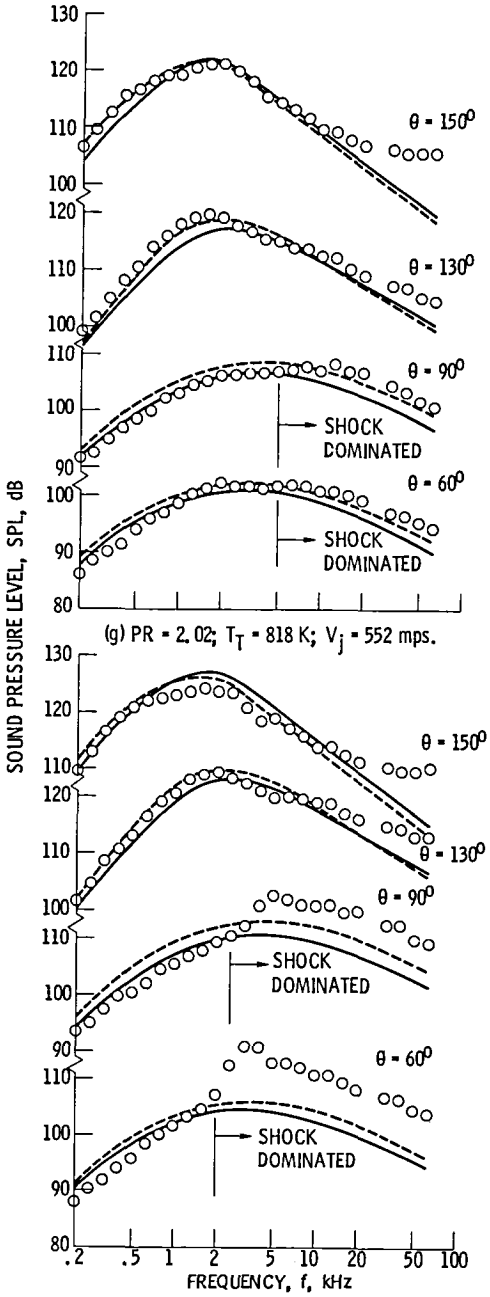

(g) PR = 2.02; T_T = 818 K; V_j = 552 mps.

(h) PR = 2.54; T_T = 817 K; V_j = 625 mps.

Figure 27. - Concluded.

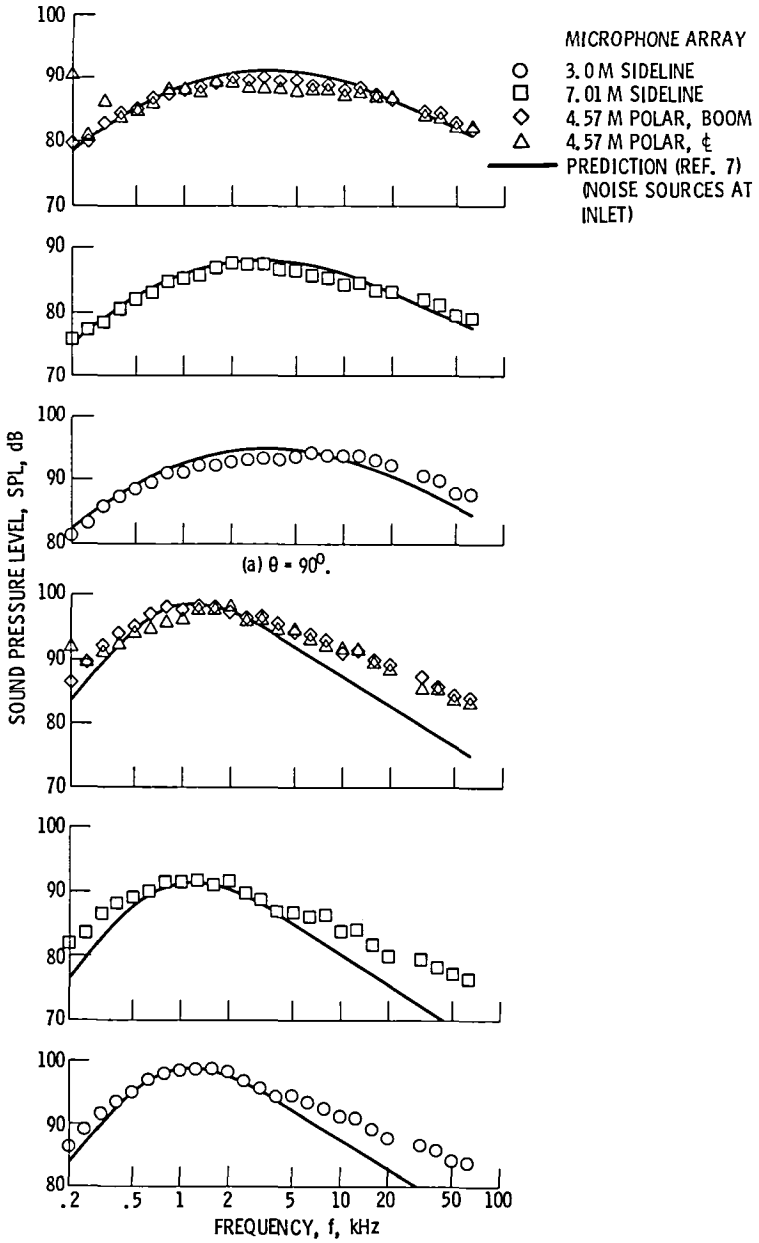

(a) $\theta = 90^0$.

(b) $\theta = 140^0$.

Figure 28. - Comparison with prediction for cold-flow spectral data for a 10.2 cm conical nozzle with different microphone arrays. PR = 1.74; T_T = 288 K; V_j = 293 mps.

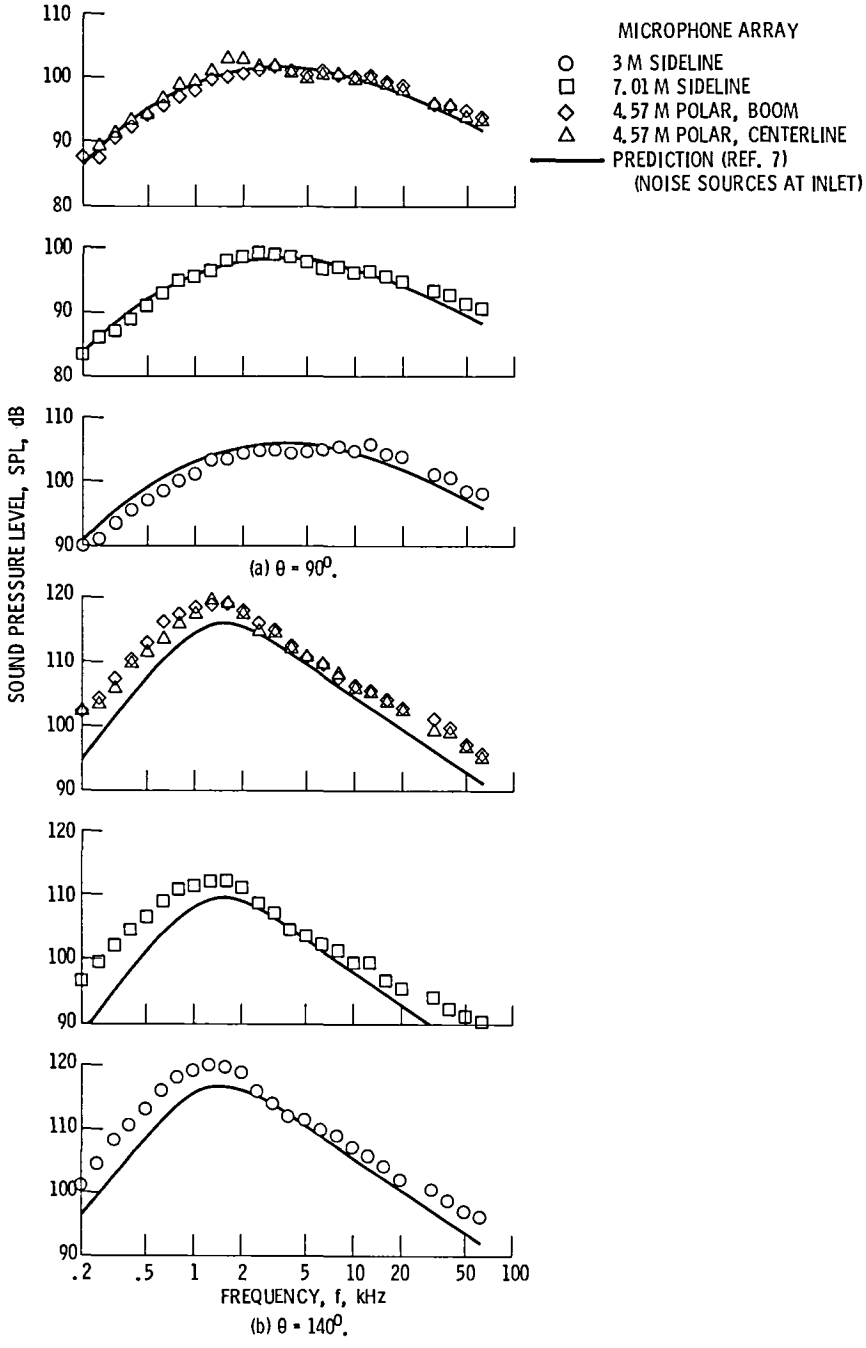

Figure 29. - Comparison with prediction for hot-flow spectral data for a 10.2 cm conical nozzle with different microphone arrays. PR = 1.75; T_T = 814 K; V_j = 498 mps.

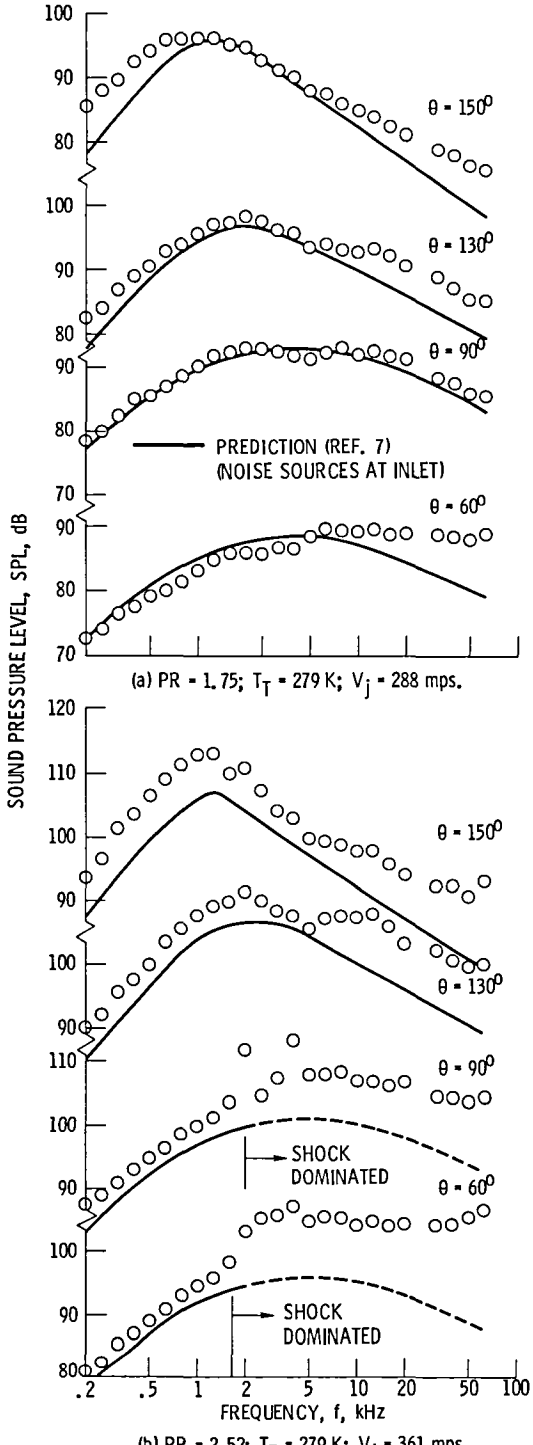

(a) PR = 1.75; T_T = 279 K; V_j = 288 mps.

(b) PR = 2.52; T_T = 279 K; V_j = 361 mps.

Figure 30. - Comparison of spectral data with prediction for the 7.6 cm conical nozzle. 3 M sideline.

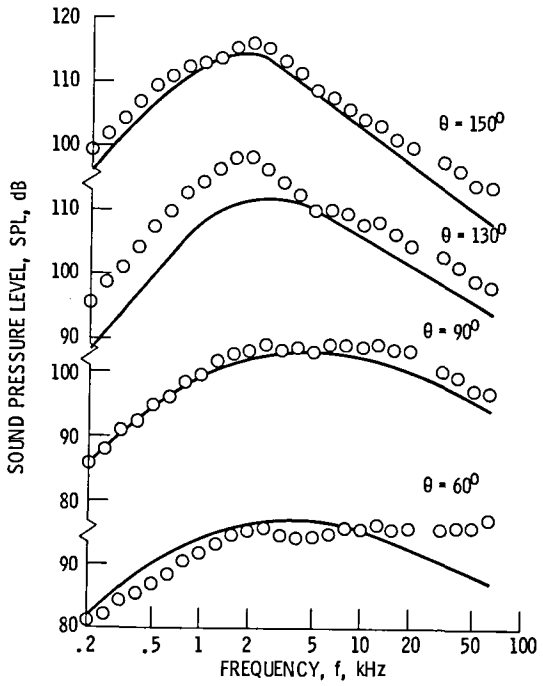

(c) PR = 1.75; T_T = 814 K; V_j = 493 mps.

Figure 30. - Concluded.

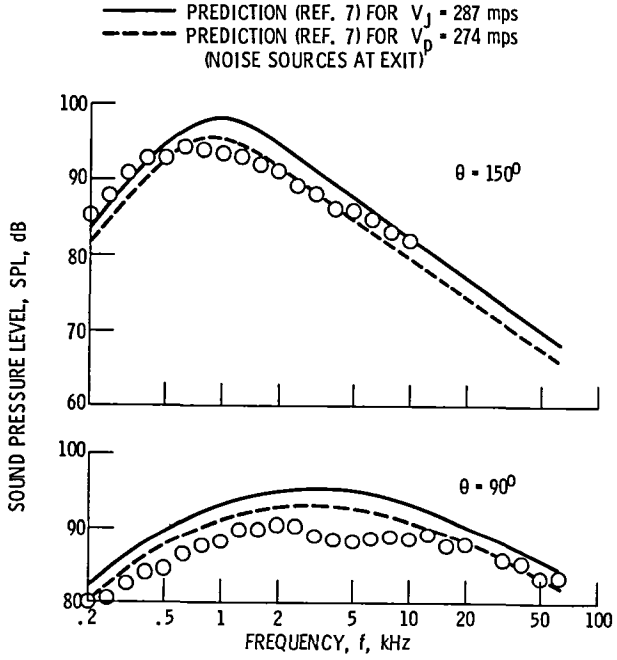

Figure 31. - Jet noise spectra for 10.2 cm conical nozzle with flow straightening screen and comparison with predictions for noise source at exit plane. PR = 1.74; T_T = 279 K.

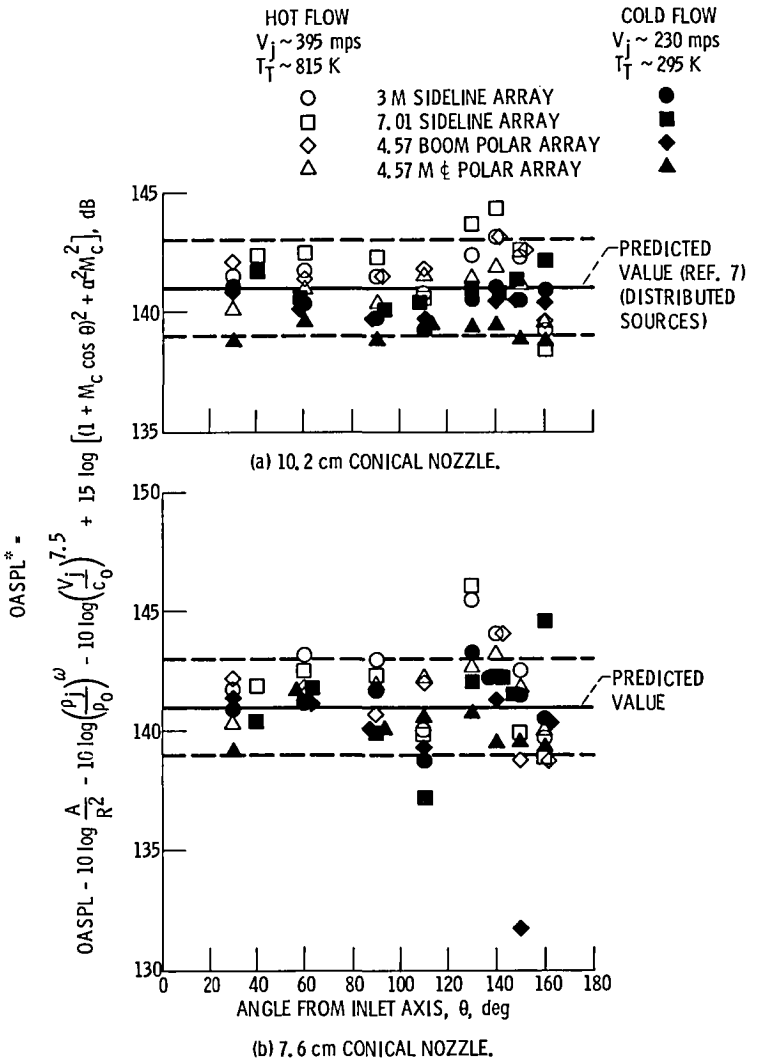

(a) 10.2 cm CONICAL NOZZLE.

(b) 7.6 cm CONICAL NOZZLE.

Figure 32. - Comparison of OASPL data with prediction for hot and cold flows; PR = 1.4.

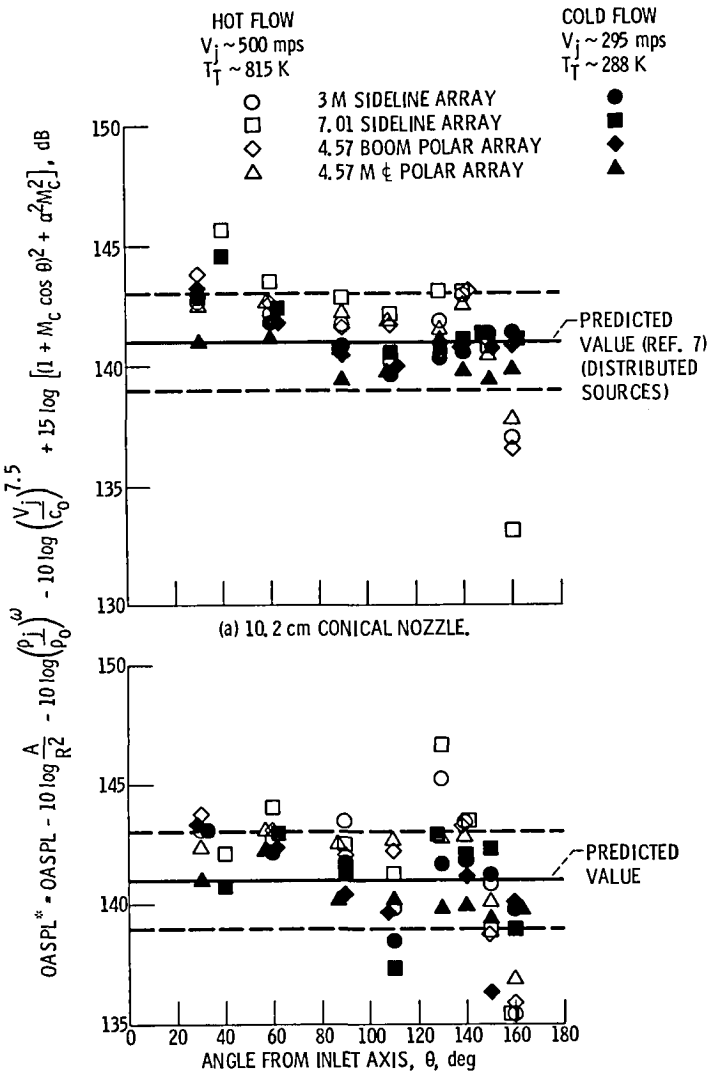

(a) 10.2 cm CONICAL NOZZLE.

(b) 7.6 cm CIRCULAR NOZZLE.

Figure 33. - Comparison of OASPL data with prediction. Hot and cold flows; PR = 1.75.

1. Report No. NASA TM-81635	2. Government Accession No.	3. Recipient's Catalog No.
4. Title and Subtitle EFFECT OF FACILITY VARIATION ON THE ACOUSTIC CHARACTERISTICS OF THREE SINGLE STREAM NOZZLES		5. Report Date 6. Performing Organization Code 505-32
7. Author(s) Orlando A. Gutierrez		8. Performing Organization Report No. E-646 10. Work Unit No.
9. Performing Organization Name and Address National Aeronautics and Space Administration Lewis Research Center Cleveland, Ohio 44135		11. Contract or Grant No. 13. Type of Report and Period Covered Technical Memorandum
12. Sponsoring Agency Name and Address National Aeronautics and Space Administration Washington, D.C. 20546		14. Sponsoring Agency Code

15. Supplementary Notes

Prepared for the One-hundredth Meeting of the Acoustical Society of America, Los Angeles, California, November 17-21, 1980.

16. Abstract

The characteristics of the jet noise produced by three single stream nozzles have been investigated statically at the NASA-Lewis Research Center outdoor jet acoustic facility. The nozzles consisted of a 7.6 cm diameter convergent conical, a 10.2 cm diameter convergent conical and an 8-lobe daisy nozzle with 7.6 cm equivalent diameter flow area. The same nozzles have been tested previously at cold flow conditions in other facilities such as the Royal Aircraft Establishment (RAE) 7.3 m acoustic wind tunnel. The acoustic experiments at NASA covered pressure ratios from 1.4 to 2.5 at total temperatures of 811 K and ambient. The data obtained with four different microphone arrays are compared. The results are also compared with data taken at the RAE facility and with a NASA prediction procedure (i.e., Stone and Montegani (1980)).

17. Key Words (Suggested by Author(s))

Acoustics; Jet noise; Single stream nozzle; Experimental results; Comparison with production

18. Distribution Statement

Unclassified - unlimited

STAR Category 71

19. Security Classif. (of this report)	20. Security Classif. (of this page)	21. No. of Pages	22. Price*
Unclassified	Unclassified		

* For sale by the National Technical Information Service, Springfield, Virginia 22161

National Aeronautics and
Space Administration

Washington, D.C.
20546

Official Business
Penalty for Private Use, $300

SPECIAL FOURTH CLASS MAIL
BOOK

Postage and Fees Paid
National Aeronautics and
Space Administration
NASA-451

NASA

POSTMASTER: If Undeliverable (Section 158
Postal Manual) Do Not Return